of an $n$-point production amplitude of the kind proposed in Ref. 26. Now the constant $C$, in (4.8), is set equal to zero and we also choose $\alpha(s)$ to be real from the outset, corresponding to a narrow-resonance approximation; this guarantees that the $n$-point model can be factorized, and that all parameters in the $n$-point amplitude can be calculated from a knowledge of the 4-point residue. In this sense, the model constitutes a "bootstrap" system with a degeneracy of states corresponding to $n^2$. Initially, the model only contains "tree" graphs, but by calculating the loop diagrams, cuts in $w(t)$ and $\alpha(s)$ will be generated, hopefully reinstating the correct analyticity properties for the 4-point function, and by summing up all the loop diagrams a complete unitarization of the scattering amplitude can be accomplished. This kind of program has been attempted for the $n$-point generalization of the Veneziano model,[27] but the simplest, single-planar dual loop constructed gives rise to an integral with an essential endpoint singularity due to the large degeneracy of the states which circulate in the loop diagram. A somewhat complicated and arbitrary procedure of renormalization has been introduced to deal with this problem.[28] In the model proposed in Ref. 26, the treatment of the diagrams follows familiar methods of Feynman graphs, and since the degeneracy of states in the model is only $n^2$, there are no divergence problems in constructing loop diagrams. Whether such a program can succeed in analogy with quantum electrodynamics is still an open question, but it is clear that a basic solution to the inelasticity problem appears to be essential in strong interactions. One interesting question arising in connection with such a method for unitarizing the model is whether the corrected trajectory will turn over at large energies, in the way assumed for the $\alpha(s)$ in our model for the 4-point amplitude, or whether it will rise indefinitely to infinity. This is the kind of fundamental question that could be answered by a basic treatment of the unitarity problem.

[26] J. W. Moffat, Nuovo Cimento Letters **2**, 773 (1969); A. O. Barut and J. W. Moffat, Phys. Rev. D **1**, 532 (1970).

[27] S. Fubini and G. Veneziano, Nuovo Cimento **64A**, 811 (1969); K. Kikkawa, B. Sakita, and M. A Virasoro, Phys. Rev. **184**, 1701 (1969).

## ACKNOWLEDGMENTS

I am grateful to several members of the High Energy Theory Group at Toronto for valuable discussions. In particular, I thank Professor R. E. Kreps and Professor R. H. Graham, and P. Curry, I. O. Moen, and V. Snell for stimulating and helpful discussions.

[28] T. H. Burnett, D. J. Gross, A. Neveu, J. Scherk, and J. H. Schwarz, Phys. Letters **32B**, 115 (1970).

PHYSICAL REVIEW D VOLUME 3, NUMBER 5 1 MARCH 1971

# Application of a Crossing-Symmetric Model Satisfying the Mandelstam Representation to $\pi$-$\pi$ and $K$-$\pi$ Scattering*

P. CURRY, I. O. MOEN, J. W. MOFFAT, AND V. SNELL
*Department of Physics, University of Toronto, Toronto, Canada*
(Received 17 July 1970)

A model for meson-meson scattering satisfying the Mandelstam representation, crossing symmetry, and Regge behavior and including a Pomeranchukon amplitude is applied to $\pi$-$\pi$ and $K$-$\pi$ scattering. Solutions are found for the $K$-$\pi$ partial waves that satisfy unitarity approximately at low energies, give a satisfactory fit to the on-mass-shell data, and predict scattering lengths consistent with current algebra. Apart from a change in the coupling constant, effectively the same parameters are then used to predict the low-energy $\pi$-$\pi$ scattering, and the solutions are found to satisfy unitarity approximately up to 900 MeV. The predicted on-mass-shell results agree well with the available data. The general conditions below threshold for $\pi$-$\pi$ scattering that follow from crossing symmetry and positivity are well satisfied. The extrapolated $\pi$-$\pi$ and $K$-$\pi$ amplitudes off the mass shell are found to agree satisfactorily with the data for $\pi N \to \pi\pi N$ and $KN \to K\pi N$ when a phenomenological form factor is used in the extrapolation. The total and differential cross sections at high energy are found to have characteristic Regge behavior. The Pomeranchukon amplitude produces total $\pi$-$\pi$ and $K$-$\pi$ cross sections consistent with factorization in the asymptotic region.

## I. INTRODUCTION

A MODEL for $\pi$-$\pi$ scattering has been developed by one of us[1] in which the scattering amplitude satisfies the following properties: (a) Mandelstam representation; (b) crossing symmetry; (c) resonances in all nonexotic channels; (d) Regge behavior in all channels; and (e) the Adler condition.

The Pomeranchukon is incorporated in the model as a nonresonant, diffractive background satisfying crossing symmetry. The Regge trajectory corresponding to the exchange-degenerate $\rho$-$f^0$ mesons is assumed to rise linearly to high energies and then turn over and tend

* Supported in part by the National Research Council of Canada.

[1] J. W. Moffat, preceding paper, Phys. Rev. D **3**, 1222 (1971). This will be referred to in the text as Paper I. See also, Nuovo Cimento **64A**, 485 (1969).

to a finite constant in the asymptotic region. In view of the nonlinear nature of this trajectory, the model has a finite number of resonances and daughters. The amplitude describes a "generalized interference" model and differs from a narrow-resonance model, such as the Veneziano model,[2] by possessing the unitarity cuts for two-body scattering corresponding to the Mandelstam representation. The Pomeranchukon amplitude, described by background cuts consistent with Mandelstam analyticity and crossing, falls naturally within the scheme of such a model, and we find that it plays an important role at low as well as high energies.

It is in the problem of spinless meson-meson scattering that we hope to find a complete solution; problems such as parity doublets in fermion-meson scattering are at present unresolved within a crossing-symmetric scheme. However, the most difficult question we are faced with is how to impose unitarity on the model while preserving crossing symmetry exactly. The difficulty arises because of the essentially nonlinear and many-body nature of the unitarity equation. If a solution of the unitarity principle can be implemented, then the model would conceivably represent a unique solution for meson-meson scattering. In Paper I, it was shown that by neglecting terms of order $m_\pi^2$, and unitarity effects, the model was consistent with the current-algebra results at threshold provided the magnitude of the scattering lengths was fixed by identifying the model with the Weinberg[3] amplitude—consistent with (e) above.

In the following, we apply the model to $\pi$-$\pi$ and $K$-$\pi$ scattering by searching for solutions that are approximately unitary at low energies. The parameters are determined by seeking absorption parameters $\eta$ that lie in the interval $0\leqslant\eta\leqslant 1$. This uniquely determines the parameters for, say, $K$-$\pi$ scattering, gives a good fit to the on-mass-shell $K$-$\pi$ data, and predicts $K$-$\pi$ scattering lengths in agreement with current algebra. With effectively the same parameters (apart from a change in the coupling constant), the $\pi$-$\pi$ scattering is then predicted and found to be approximately unitary up to 900 MeV, and to provide a good description of the available low-energy data; the scattering lengths are in close agreement with current algebra and chiral $SU(2)\otimes SU(2)$. The general conditions on $\pi^0$-$\pi^0$ scattering obtained by several authors below threshold are well satisfied.

Because the calculations performed are only valid at low energies—below the $f^0$ meson—or at high energies where unitarity is not crucial, we included only one satellite term. In order to extend these calculations to the intermediate energy range, we must include the $\omega\pi$, $K\bar{K}$, and $N\bar{N}$ coupled channels and further satellites. No attempt is made to carry out such a program in this paper. We used the low-energy parameters to predict the high-energy $\pi$-$\pi$ and $K$-$\pi$ scattering, including the effects of the Pomeranchukon, and find total cross sections of the expected magnitude in the asymptotic region and differential cross sections with the characteristic Regge behavior. Thus, low- and high-energy meson-meson scattering are provided a unified description within the model. A complete solution of the problem must await a satisfactory treatment of the difficult intermediate resonance region.

The processes $\pi N\to\pi\pi N$ and $KN\to K\pi N$ are studied by extrapolating the $\pi$-$\pi$ and $K$-$\pi$ amplitudes off the mass shell. In terms of a phenomenological form factor, good fits to the data are obtained for the Chew-Low extrapolations of the total and the differential cross sections; also the on-mass-shell forward-backward asymmetry is well fitted.

The paper is organized as follows. In Sec. II, the kinematics and amplitudes for $\pi$-$\pi$ and $K$-$\pi$ scattering are discussed; in Sec. III, the specific model for the Pomeranchukon amplitude is presented. In Sec. IV, the parameters for $K$-$\pi$ scattering are determined by our unitarization procedure and the results are compared with the data. The calculations for $\pi$-$\pi$ scattering are then presented in Sec. V and the results are compared with the low-energy data. In Sec. VI, the positivity and crossing conditions below threshold are studied, and in Sec. VII, the off-mass-shell calculations are described for both $\pi N\to\pi\pi N$ and $KN\to K\pi N$ scattering. The high-energy scattering predicted by the model is then discussed in Sec. VIII. Finally, in Sec. IX, we end the paper with concluding remarks.

## II. KINEMATICS AND SCATTERING AMPLITUDES

We summarize for the sake of completeness the basic kinematical notation and properties of the amplitudes discussed in Paper I. Let us define the $T$ matrix in terms of the $S$ matrix by

$$S_{fi}=\delta_{fi}+i(2\pi)^4\delta(p_f-p_i)T_{fi} \tag{2.1}$$

and the scattering amplitude $f(s,\theta)$ by

$$f(s,\theta)=(1/8\pi\sqrt{s})T. \tag{2.2}$$

The isotopic-spin amplitudes $f^I(s,\theta)$ can be expanded in a sum over partial waves:

$$f^I(s,\theta)=\sum_{l=0}^{\infty}(2l+1)f_l{}^I(s)P_l(\cos\theta), \tag{2.3}$$

with

$$f_l{}^I(s)=\frac{1}{2}\int_{-1}^{1}f^I(s,\theta)P_l(\cos\theta)d\cos\theta. \tag{2.4}$$

In $\pi$-$\pi$ scattering, the partial-wave expansion of the

[2] G. Veneziano, Nuovo Cimento **57A**, 190 (1968).
[3] S. Weinberg, Phys. Rev. Letters **17**, 616 (1966).

isotopic-spin amplitudes is

$$f^I(s,\theta)=\sum_{l=0}^{\infty}(2l+1)f_l{}^I(s)P_l(\cos\theta)[1+(-1)^{l+I}], \quad (2.5)$$

where the extra factor is due to Bose statistics.

We unitarize the partial waves $f_l{}^I(s)$ and set

$$f_l{}^I(s)=\frac{1}{2iq}(\eta_l{}^I e^{2i\delta_l{}^I}-1), \quad (2.6)$$

which implies that the elastic unitarity equation (for the absorption parameter $\eta$ equal to unity) is

$$\mathrm{Im}f_l{}^I(s)=q|f_l{}^I(s)|^2. \quad (2.7)$$

The total invariant amplitude is defined by

$$A^I(s,t,u)=F_{\rho,K^*}{}^I(s,t,u)+P^I(s,t,u), \quad (2.8)$$

where $F_\rho{}^I$ and $F_{K^*}{}^I$ denote the amplitudes for $\pi$-$\pi$ and $K$-$\pi$ scattering, corresponding to $\rho$, $f$ and $K^*$, $K^{**}$ exchanges, respectively, while $P^I$ denotes the Pomeranchukon amplitude.

Amplitudes of definite isospin for $\pi$-$\pi$ scattering are determined in the $s$ channel by[1,4]

$$\begin{aligned}
A_s{}^{I=0}&=\tfrac{3}{2}[F_\rho(s,t)+F_\rho(s,u)]-\tfrac{1}{2}F_\rho(t,u)\\
&\quad+A_P(t,s)+A_P(t,u)+A_P(u,s)\\
&\quad+A_P(u,t)+3[A_P(s,t)+A_P(s,u)],\\
A_s{}^{I=1}&=F_\rho(s,t)-F_\rho(s,u)+A_P(t,s)\\
&\quad+A_P(t,u)-A_P(u,s)-A_P(u,t),\\
A_s{}^{I=2}&=F_\rho(t,u)+A_P(t,u)\\
&\quad+A_P(t,s)+A_P(u,s)+A_P(u,t),
\end{aligned} \quad (2.9)$$

where $F_\rho(s,t)=F_\rho(t,s)$. Then various charged-pion processes are given by

$$\begin{aligned}
\{\pi^0\pi^0\to\pi^0\pi^0\}&=\tfrac{1}{3}A^0+\tfrac{2}{3}A^2,\\
\{\pi^+\pi^-\to\pi^+\pi^-\}&=\tfrac{1}{3}A^0+\tfrac{1}{2}A^1+\tfrac{1}{6}A^2,\\
\{\pi^\pm\pi^0\to\pi^\pm\pi^0\}&=\tfrac{1}{2}(A^1+A^2),\\
\{\pi^+\pi^-\to\pi^0\pi^0\}&=\tfrac{1}{3}(A^2-A^0),\\
\{\pi^\pm\pi^\pm\to\pi^\pm\pi^\pm\}&=A^2.
\end{aligned} \quad (2.10)$$

The scattering amplitude is related to the $\pi$-$\pi$ invariant isospin amplitude $A^I$ by

$$f^I(s,\theta)=(1/16\pi\sqrt{s})A^I(s,t,u). \quad (2.11)$$

In $K$-$\pi$ scattering there are two values of the isospin $I=\frac{1}{2}$ and $I=\frac{3}{2}$ in the $s$ and $u$ channels. The absence of exotic resonances in the $I=\frac{3}{2}$ channel permits us to write in the $s$ channel

$$F_s{}^{I=3/2}=F_{K^*}(u,t),$$

where $F_{K^*}(s,t)=F_{K^*}(t,s)$. The amplitude $F_s{}^{I=1/2}$ is uniquely determined by $s$-$u$ crossing symmetry to be

$$F_s{}^{I=1/2}=\tfrac{3}{2}F_{K^*}(s,t)-\tfrac{1}{2}F_{K^*}(u,t). \quad (2.12)$$

Let us consider the Pomeranchukon isospin amplitudes. We demand, as in $\pi$-$\pi$ scattering, that the Pomeranchukon is an $I=0$ object and, therefore, $P^{I=1/2}(s,t)$ and $P^{I=3/2}(s,t)$ must have no poles in $s$. The most general form we may write for $P^{I=3/2}$ is

$$\begin{aligned}
P^{I=3/2}&=aA_P(t,u)+bA_P(u,t)\\
&\quad+cA_P(u,s)+dA_P(t,s).
\end{aligned} \quad (2.13)$$

Then $P^{I=1/2}$ is determined from crossing symmetry to be

$$\begin{aligned}
P^{I=1/2}&=\tfrac{3}{2}[aA_P(t,s)+bA_P(s,t)\\
&\quad+cA_P(s,u)+dA_P(t,u)]\\
&\quad-\tfrac{1}{2}[aA_P(t,u)+bA_P(u,t)\\
&\quad+cA_P(u,s)+dA_P(t,s)].
\end{aligned} \quad (2.14)$$

Absence of poles in $P^{I=1/2}$ implies that $b=c=0$. Consequently,

$$\begin{aligned}
P^{I=1/2}&=(\tfrac{3}{2}a-\tfrac{1}{2}d)A_P(t,s)+(\tfrac{3}{2}d-\tfrac{1}{2}a)A_P(t,u),\\
P^{I=3/2}&=aA_P(t,u)+dA_P(t,s).
\end{aligned} \quad (2.15)$$

The Pomeranchuk theorem demands that $P^{I=1/2}=P^{I=3/2}$ at asymptotic energies. Therefore, $a=d$, and absorbing the remaining constant into $A_P$, we get in the $s$ channel

$$\begin{aligned}
P_s{}^{I=1/2}&=P_s{}^{I=3/2}\\
&=A_P(t,s)+A_P(t,u).
\end{aligned} \quad (2.16)$$

The crossing matrix relating $s$ and $t$ channels is

$$\begin{pmatrix}P_t{}^{I=0}\\ P_t{}^{I=1}\end{pmatrix}=\begin{pmatrix}\frac{1}{2}\sqrt{6} & \sqrt{6}\\ 1 & -1\end{pmatrix}\begin{pmatrix}P_s{}^{I=1/2}\\ P_s{}^{I=3/2}\end{pmatrix}. \quad (2.17)$$

Applying crossing gives

$$P_t{}^{I=1}=0$$

and

$$P_t{}^{I=0}=\tfrac{3}{2}\sqrt{6}[A_P(t,s)+A_P(t,u)]. \quad (2.18)$$

Thus the total isospin amplitudes in $K$-$\pi$ scattering in the $s$ channel are

$$\begin{aligned}
A^{I=1/2}&=\tfrac{3}{2}F_{K^*}(s,t)-\tfrac{1}{2}F_{K^*}(u,t)\\
&\quad+A_P(t,s)+A_P(t,u),\\
A^{I=3/2}&=F_{K^*}(u,t)+A_P(t,s)+A_P(t,u).
\end{aligned} \quad (2.19)$$

In $K$-$\pi$ scattering the invariant amplitude is related to the scattering amplitude by

$$f^I(s,\theta)=(1/8\pi\sqrt{s})A^I(s,t,u). \quad (2.20)$$

In the model[1] the amplitudes $F_\rho(s,t)$ and $F_{K^*}(s,t)$, including the first satellite, are given by

$$\begin{aligned}
F_\rho(s,t)&=-\gamma_\rho(s)\Gamma(1-\alpha_\rho(s))\\
&\quad\times[w_\rho(t)^{\alpha_\rho(s)}+d_1w_{1\rho}(t)^{\alpha_\rho(s)-1}]+(s\leftrightarrow t),
\end{aligned} \quad (2.21)$$

[4] J. Shapiro and J. Yellin, Yadern. Fiz. **11**, 443 (1970) [Soviet J. Nucl. Phys. **11**, 247 (1970)]; J. Shapiro, Phys. Rev. **179**, 1345 (1969); A. Yahil, *ibid.* **185**, 1787 (1969); C. Lovelace, Phys. Letters **28B**, 265 (1968); E. Del Guidice and G. Veneziano, Nuovo Cimento Letters **3**, 363 (1970).

where the nonlinear trajectory $\alpha_\rho(s)$, corresponding to $\rho$-$f^0$ exchange, is given by

$$\alpha_\rho(s)=a_\rho+\frac{bs-c_\rho(4m_\pi^2-s)^{1/2}}{\{1+[(4m_\pi^2-s)/\Delta]^{1/2}\}^2}. \quad (2.22)$$

The condition $\mathrm{Re}\alpha_\rho(m_\rho^2)=1$, the Adler[5] condition $\alpha_\rho(m_\pi^2)=\frac{1}{2}$, and a knowledge of the total widths of the $\rho$, $f^0$, and $g$ mesons gives $a=0.51$, $b=0.838$ GeV$^{-2}$, $c_\rho=0.107$ GeV$^{-1}$, $\Delta^{1/2}=100$ GeV; this leads to the intercept $\alpha_\rho(0)=0.48$. Moreover,

$$\gamma_\rho(s)=\frac{\gamma[\alpha_\rho(s)-\frac{1}{2}]\exp[-g\alpha_\rho{}^2(s)]}{[1+x_\rho(s)]^{2q}}, \quad (2.23)$$

where

$$x_\rho(s)=(4m_\pi^2-s)^{1/2}/\Lambda. \quad (2.24)$$

The constants $\gamma$, $g$, $\Lambda$, and $q$ are positive and $\Lambda$ is chosen large; in the calculations the specific choices of $\Delta$ and $\Lambda$ are unimportant. The function $w_\rho(s)$ is given by

$$w_\rho(s)=A+Bs+C(16m_\pi^2-s)^{1/2}. \quad (2.25)$$

As explained in Paper I, the analyticity requirements demand that $A>0$, $B<0$, and $C>0$. The function $w_{1\rho}(s)$ associated with the satellite term will differ from $w_\rho(s)$ because of the constant $A$. As the function $\gamma_\rho(s)=0$ at $s=m_\pi^2$, it follows that $F_\rho(m_\pi^2,m_\pi^2)=0$ and the Adler condition is satisfied.

The amplitude $F_{K^*}(s,t)$ is given by

$$\begin{aligned}F_{K^*}(s,t)=&-\gamma_{K^*}(s)\Gamma(1-\alpha_{K^*}(s))\\&\times[w_\rho(t)^{\alpha_{K^*}(s)}+d_1w_{1\rho}(t)^{\alpha_{K^*}(s)-1}]\\&-\gamma_\rho(t)\Gamma(1-\alpha_\rho(t))\\&\times[w_{K^*}(s)^{\alpha_\rho(t)}+d_1w_{1K^*}(s)^{\alpha_\rho(t)-1}]. \quad (2.26)\end{aligned}$$

The trajectory $\alpha_{K^*}(s)$ is

$$\alpha_{K^*}(s)=a_{K^*}+\frac{bs-c_{K^*}[(m_K+m_\pi)^2-s]^{1/2}}{\{1+[((m_K+m_\pi)^2-s)/\Delta]^{1/2}\}^2}. \quad (2.27)$$

The conditions $\mathrm{Re}\alpha_{K^*}(m_{K^*}{}^2)=1$, $\alpha_{K^*}(m_K{}^2)=\frac{1}{2}$ and the knowledge of the total width of the $K^*$ resonance determine the constants to be $a_{K^*}=0.314$, $c_{K^*}=0.061$ GeV$^{-1}$, and $\alpha_{K^*}(0)=0.28$. Moreover,

$$\gamma_{K^*}(s)=\frac{\gamma[\alpha_{K^*}(s)-\frac{1}{2}]\exp[-g\alpha_{K^*}{}^2(s)]}{[1+x_{K^*}(s)]^{2q}}, \quad (2.28)$$

where

$$x_{K^*}(s)=[(m_K+m_\pi)^2-s]^{1/2}/\Lambda. \quad (2.29)$$

At the point $s=u=m_K{}^2$ the trajectory satisfies $\alpha_{K^*}(m_K{}^2)=\frac{1}{2}$ and $\gamma_{K^*}(m_K{}^2)=0$, so that $F_{K^*}(m_K{}^2,m_\pi{}^2)=0$ and the Adler condition is satisfied. The function $w_{K^*}(s)$ is given by

$$w_{K^*}(s)=A+Bs+C[(m_K+2m_\pi)^2-s]^{1/2}, \quad (2.30)$$

where the cut begins at the first inelastic threshold $(m_K+2m_\pi)^2$. The function $w_{1K^*}(s)$ associated with the satellite term will differ from $w_{K^*}(s)$ by virtue of the parameter $A$. The same parameter $B$ is used in both processes and is chosen to be the negative of the universal Regge slope 0.84 GeV$^{-2}$. This gives the correct $s$ dependence of the amplitude at high energy, $(-s/s_0)^{\alpha(t)}$, as $|B|=1/s_0$.

## III. MODEL FOR POMERANCHUKON AMPLITUDE

The requirements for a model of the Pomeranchukon amplitude were discussed in Paper I. However, we find it more convenient to use an alternative model for $A_P(s,t)$ in the present calculations. We must include the Pomeranchukon contributions to the $\pi$-$\pi$ and $K$-$\pi$ scattering for two main reasons:

(1) A Pomeranchukon is exchanged in the $t$ channel with $I=0$ in both $\pi$-$\pi$ and $K$-$\pi$ scattering; hence it contributes a dominant term in the $s$-channel total cross sections at asymptotic energies;

(2) In $\pi$-$\pi$ scattering, the $s$-channel amplitude $F_\rho{}^{I=2}$ (and in $K$-$\pi$ scattering the $s$-channel amplitude $F_{K^*}{}^{I=3/2}$) is purely real for all $s$ above threshold. This implies that there is no scattering in these channels if unitarity is satisfied, and this prediction is obviously wrong. Thus, the Pomeranchukon must contribute an imaginary part to these channels.

Let us consider the properties that our model for the Pomeranchukon amplitude must satisfy:

(i) Unitarity demands that it have a positive imaginary part in all partial waves from threshold, $s=R$, to infinity [where $R=4m_\pi{}^2$ for $\pi$-$\pi$ scattering and $R=(m_K+m_\pi)^2$ for $K$-$\pi$ scattering].

(ii) The imaginary part must be zero at threshold.

(iii) The Pomeranchukon amplitude for any isospin must become purely imaginary at high energies, and must behave like $(s/s_0)^{\alpha_P(t)}$ as $s\to\infty$, where $s_0\sim 1$ GeV$^2$ and $\alpha_P(t)$ is the Pomeranchukon trajectory.

(iv) The Pomeranchukon amplitude must satisfy the Adler condition for both $\pi$-$\pi$ and $K$-$\pi$ scattering.

(v) It should have Mandelstam analyticity; in particular, it should be cut in the region $R\leqslant s\leqslant\infty$ and should satisfy a dispersion relation.

Let us now proceed to derive $A_P(t,s)$. We require that

$$\mathrm{Im}A_P(t,s)\sim(s-R)(s/s_0)^{\alpha_P(t)-1}. \quad (3.1)$$

We assume that $A_P(t,s)$ satisfies a twice-subtracted dispersion relation

$$A_P(t,s)=\gamma_P\left[D+K(s-m_0^2)+\frac{s^2}{\pi}\int_R^\infty\frac{x-R}{x}\left(\frac{x}{s_0}\right)^{\alpha_P(t)}\frac{dx}{x^2(x-s)}\right], \quad (3.2)$$

[5] S. L. Adler, Phys. Rev. **137**, B1022 (1965); **139**, B163 (1965); **140**, B736 (1965).

where $D$ and $K$ are the subtraction constants. In fact

$$A_P(t,0)=D-Km_0^2,\qquad A_P'(t,0)=K, \tag{3.3}$$

where $m_0=m_\pi$ for $\pi$-$\pi$ scattering and $m_0=m_K$ for $K$-$\pi$ scattering. Then the Adler point corresponds to $s=m_0^2$. Note that we have the option of making $D$ and $K$ functions of $t$; however, this will not be required in our work.

The Pomeranchukon trajectory is given by

$$\alpha_P(t)=1+\frac{b_P t}{\{1+[(16m_\pi^2-t)/\Delta]^{1/2}\}^2}. \tag{3.4}$$

We choose $b_P$ to be the universal value $b_P=b=0.85$ GeV$^{-2}$. The turnover point $s_T=\Delta$ is chosen to be the same as for the $\rho$-$f^0$ trajectory: $\Delta^{1/2}=100$ GeV. We find that the calculations are insensitive to both $b$ and $\Delta$; for example, a change in $b$ from 0.4 GeV$^{-2}$ to 0.8 GeV$^{-2}$ changes the low-energy phase shifts by less than 10%.

In order to evaluate the integral (3.2), we let $1/y=x/R$. Then

$$A_P(t,s)=\gamma_P\left[D+K(s-m_0^2)+R^{\alpha_P(t)-2}\left(\frac{1}{s_0}\right)^{\alpha_P(t)}\frac{s^2}{\pi}\times\int_0^1(1-y)\left(1-\frac{s}{R}y\right)^{-1}y^{1-\alpha_P(t)}dy\right]. \tag{3.5}$$

This is the integral representation for the hypergeometric function

$$\frac{\Gamma(b)\Gamma(c-b)}{\Gamma(c)}F(a;b;c,s)=\int_0^1 t^{b-1}(1-t)^{c-b-1}(1-ts)^{-a}dt, \tag{3.6}$$

where $\mathrm{Re}c>\mathrm{Re}b>0$. The latter restriction implies $\alpha_P<2$, but this will be removed as discussed below. Thus, we have

$$A_P(t,s)=\gamma_P\left[D+K(s-m_0^2)+\frac{R^{\alpha_P(t)-2}s^2}{\pi s_0^{\alpha_P(t)}}\frac{F(1;2-\alpha_P(t);4-\alpha_P(t),s/R)}{[2-\alpha_P(t)][3-\alpha_P(t)]}\right]. \tag{3.7}$$

There are simple poles in (3.7) as a function of $t$ for $\alpha_P(t)=2,3,\ldots$. Since no resonances have been observed on the Pomeranchukon trajectory, we remove these by dividing $F$ by $\Gamma(2-\alpha_P(t))$. $F$ is cut in $s$ in the region $R\leqslant s\leqslant\infty$ and our representation above, including the factor of $1/\Gamma(2-\alpha_P(t))$, holds for all $\alpha_P$ and all $s$.

The evaluation of the hypergeometric function is quite straightforward. For $|s|<R$, $F$ can be written as a rapidly convergent Gauss series and $A_P(t,s)$ becomes

$$A_P(t,s)=\gamma_P\left\{D+K(s-m_0^2)+\frac{1}{\Gamma(2-\alpha_P(t))}\left(\frac{R^{\alpha_P(t)-2}}{s_0^{\alpha_P(t)}}\right)\frac{s^2}{\pi}\times\left[\sum_{n=0}^{\infty}\frac{1}{[3-\alpha_P(t)+n][2-\alpha_P(t)+n]}\left(\frac{s}{R}\right)^n\right]\right\}. \tag{3.8}$$

For $|s|=R$, this sum can be performed explicitly. By using

$$F(\alpha;\beta;\gamma,1)=\frac{\Gamma(\gamma)\Gamma(\gamma-\alpha-\beta)}{\Gamma(\gamma-\alpha)\Gamma(\gamma-\beta)}, \tag{3.9}$$

we get

$$A_P(t,R)=\gamma_P\left[D+K(R-m_0^2)+\frac{1}{\pi}\frac{1}{\Gamma(3-\alpha_P(t))}\left(\frac{R}{s_0}\right)^{\alpha_P(t)}\right]. \tag{3.10}$$

Finally, for $|s|>R$, we use the transformation formula

$$F(a;b;c,z)=\frac{\Gamma(c)\Gamma(b-a)}{\Gamma(b)\Gamma(c-a)}(-z)^{-a}F\left(a;1-c+a;1-b+a,\frac{1}{z}\right)+\frac{\Gamma(c)\Gamma(a-b)}{\Gamma(a)\Gamma(c-b)}(-z)^{-b}F\left(b;1-c+b;1-a+b,\frac{1}{z}\right) \tag{3.11}$$

to perform the analytic continuation. By using the Gauss series again, we evaluate these new hypergeometric series ($|1/z|<1$):

$$A_P(t,s)=\gamma_P\left\{D+K(s-m_0^2)+\frac{1}{\Gamma(2-\alpha_P(t))}\frac{1}{\pi}\left(\frac{R}{s_0}\right)^{\alpha_P(t)}\times\left[-\left(\frac{s}{R}\right)\sum_{n=0}^{\infty}\frac{1}{(\alpha-1+n)(\alpha-2+n)}\left(\frac{R}{s}\right)^n-\frac{\pi}{\sin\pi\alpha_P(t)}\left(\frac{-s}{R}\right)^{\alpha_P(t)}\left(1-\frac{R}{s}\right)\right]\right\}. \tag{3.12}$$

The cut in $A_P(t,s)$ is explicit in the term $(-s/R)^{\alpha_P(t)}$.

The above formula is valid for all values of $\alpha_P(t)$, including integer values; actually to show that the apparent poles at $\alpha_P=-m$ ($m=-1,0,+1,2,\ldots$) do not occur, we simply take the limit of the expression

as $\alpha_P \to -m$, to give

$$A_P(t,s)=\gamma_P\Big\{D+K(s-m_0^2)+\frac{1}{\Gamma(m+2)}\Big(\frac{s_0^m}{R^m}\Big)\frac{1}{\pi}\Big[-\Big(\frac{s}{R}\Big)\Big\{\Big[\sum_{n=0}^{m}+\sum_{n=m+3}^{\infty}\Big]\times\frac{1}{(n-m-1)(n-m-2)}\Big(\frac{R}{s}\Big)^n-\Big(\frac{R}{s}\Big)^{m+1}-\Big(\frac{R}{s}\Big)^{m+2}\Big\}+i\pi\Big(\frac{R}{s}\Big)^m\Big(1-\frac{R}{s}\Big)\Big]-\frac{R}{\pi s^{m+1}}\Big(\frac{s}{R}-1\Big)\ln\Big|\frac{s}{R}\Big|\Big\}. \quad (3.13)$$

Asymptotically, we have for $s\to\infty$ and fixed $t$

$$A_P(t,s)\approx\gamma_P\Big\{Ks+\frac{1}{\Gamma(2-\alpha_P(t))}\frac{1}{\pi}\Big(\frac{R}{s_0}\Big)^{\alpha_P(t)}\times\Big[-\Big(\frac{s}{R}\Big)\frac{1}{\alpha_P(t)[\alpha_P(t)-1]}-\frac{\pi}{\sin\pi\alpha_P(t)}\times\Big(\frac{-s}{R}\Big)^{\alpha_P(t)}\Big(1-\frac{R}{s}\Big)\Big]\Big\}. \quad (3.14)$$

We recall that as $\alpha_P \to$ integer, the lower-order terms in the sum cancel the apparent poles. In $\pi$-$\pi$ scattering in order to increase the convergence to the Regge asymptotic limit, we multiply the Pomeranchukon amplitude by an over-all function,

$$A_P(t,s)\to\frac{e^{-\alpha_P^2(t)}}{\{1+[(16m_\pi^2-t)/\Lambda]^{1/2}\}^{2q}}A_P(t,s)=\gamma_P(t)A_P(t,s), \quad (3.15)$$

where $\Lambda$ and $q$ are the same as in Eqs. (2.23) and (2.28). Now $A_P(t,s)$ goes to zero for large values of $t$. This means that for $\pi$-$\pi$ scattering, in the $s$ channel, for $s\to\infty$ and fixed $t$, we get

$$P^I\sim A_P(t,s)+A_P(t,u), \quad (3.16)$$

whereas for $K$-$\pi$ scattering, we recall that

$$P^{I=1/2}=P^{I=3/2}=A_P(t,s)+A_P(t,u) \quad (3.17)$$

is satisfied exactly. Thus, the common Pomeranchukon contribution to all isospin amplitudes in the $s$ channel for $s\to\infty$ and fixed $t$, in both $\pi$-$\pi$ and $K$-$\pi$ scattering is

$$P^I\sim\frac{\gamma_P(t)}{\Gamma(2-\alpha_P(t))}\Big(\frac{s}{s_0}\Big)^{\alpha_P(t)}\Big(\frac{1+e^{-i\pi\alpha_P(t)}}{\sin\pi\alpha_P(t)}\Big). \quad (3.18)$$

The trajectory $\alpha_P(t)$ has the asymptotic value

$$\alpha_P(\pm\infty)=1-b\Delta\approx-b\Delta. \quad (3.19)$$

The appearance of a signature factor in the $s$-channel amplitudes is a reflection of the fact that the Pomeranchukon is an $I=0$ object exchanged in the $t$ channel.

It can easily be shown that because $\alpha_P(t)$ has the negative constant asymptotic value (3.19), the Pomeranchukon amplitude does not violate the Cerulus-Martin bound $\exp[-\sqrt{|s|}C(t)]$ [$C(t)$ a slowly varying function of $t$] for large-angle scattering, $s\to\infty$ and $t\to-\infty$ ($u$ fixed).

We choose the subtraction and coupling constants as follows: The coupling constant $\gamma_P$ is chosen to give the correct magnitude of the total cross sections from factorization arguments; this also gives the correct $I=2$ amplitude at low energies. The subtraction constant $K$ is chosen to give the $I=2$ ($I=\frac{3}{2}$ for $K\pi$) phase shift at low energies, and $D$ is then calculated to give the Adler condition

$$P^I(s,t,u)\big|_{s=u=m_K^2;\,t=m_\pi^2}=0 \quad (K\text{-}\pi \text{ scattering}),$$
$$P^I(s,t,u)\big|_{s=t=u=m_\pi^2}=0 \quad (\pi\text{-}\pi \text{ scattering}). \quad (3.20)$$

However, the basic restriction on the parameters $\gamma_P$, $D$, and $K$ arises from the unitarization procedure in low-energy scattering.

## IV. RESULTS FOR $K$-$\pi$ SCATTERING ON THE MASS SHELL

Let us begin our description of the results of the application of the model with $K$-$\pi$ scattering. We unitarize the partial waves by considering the absorption parameters

$$|\eta_l^I|=|1+2iqf_l^I(s)|. \quad (4.1)$$

Here $q$ is the magnitude of the c.m. 3-momentum

$$q=\frac{1}{2\sqrt{s}}(s^2+m_K^4+m_\pi^4-2sm_\pi^2-2sm_K^2-2m_\pi^2m_K^2)^{1/2} \quad (4.2)$$

and the relationship between $s,t$, and the c.m. scattering

TABLE I. Values of parameters calculated from unitarity considerations.

| Name | Description of parameter | Parameters calculated from unitarity |
|---|---|---|
| $\gamma$ | Over-all coupling constant | 167 (for $\pi\pi$)<br>124 (for $K\pi$) |
| $g$ | Exponential dependence of amplitudes $F_\rho$ and $F_{K^*}$ | 0.3 |
| $A$ | Leading constant in $w_{K^*}(t)$, $w_\rho(t)$ | 2 72 |
| $A_1$ | Leading constant in satellite function $w_{1K^*}(t)$, $w_{1\rho}(t)$ | 2.28 |
| $d_1$ | Satellite coefficient | $-3.01$ (for $\pi\pi$)<br>$-2.96$ (for $K\pi$) |
| $C$ | Square-root coefficient in $w_{K^*}(t)$ and $w_{1K^*}(t)$ | 0.086 GeV$^{-1}$ |
| $\gamma_P$ | Pomeranchukon coupling constant | 0.60 |
| $K$ | Pomeranchukon subtraction constant | $-1.28$ GeV$^{-2}$ |

angle $\theta$ is

$$\cos\theta=\frac{s^2+2s(t-m_K^2-m_\pi^2)+(m_K^2-m_\pi^2)^2}{s^2+m_K^4+m_\pi^4-2sm_K^2-2sm_\pi^2-2m_K^2m_\pi^2}. \quad (4.3)$$

The $S$-wave scattering lengths are defined by

$$a_I=\lim_{s\to(m_K+m_\pi)^2}\delta_{l=0}{}^I(s)/q. \quad (4.4)$$

The parameters are determined by demanding elastic unitarity $\eta_l{}^I=1$ in all partial waves in the region

$$(m_K+m_\pi)^2\leqslant s\leqslant(m_K+2m_\pi)^2$$

and nonviolation of unitarity $\eta_l{}^I\leqslant 1$ above the first inelastic threshold. This procedure determines the values of the parameters shown in Table I. The $I=\frac{1}{2}$ $S$ wave depends almost entirely on the leading term and not on the satellite and Pomeranchukon terms in the low-energy region. Consequently, $\gamma$ is determined by setting $\eta_0{}^{1/2}=0.83$ at the mass of the $K^*$ resonance. Unitarity determinations of $\eta_l{}^I$ are found to be very insensitive to $C$ provided $C$ is small. It is necessary that $C$ be small in order to avoid high-spin "ancestors."[1] The contribution of the ancestors at the poles is $<5\%$ for the unitarized solutions. The constants $\gamma_P$ and $K$ are determined principally by unitarity in the $I=\frac{3}{2}$ $S$ wave, although the Pomeranchukon also contributes to the $I=\frac{1}{2}$ $S$ wave. The unitarization procedure is sensitive to variations in $d_1$. The Pomeranchukon subtraction constant $D$ is determined by the $K$-$\pi$ Adler condition to be $-2.55\times10^{-2}$.

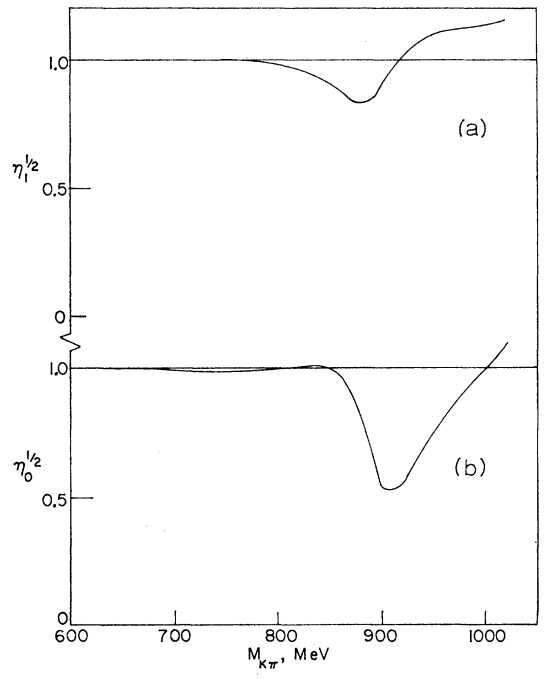


FIG. 1. (a) Absorption parameter $\eta_{l=1}{}^{I=1/2}$ as a function of the $K\pi$ mass. (b) $\eta_{l=0}{}^{I=1/2}$.

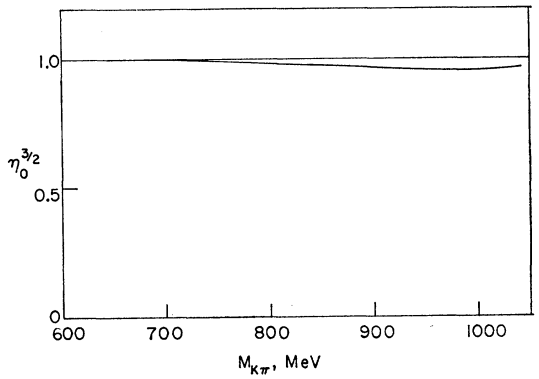


FIG. 2. Absorption parameter $\eta_{l=0}{}^{I=3/2}$.

The $\eta_l{}^I$ determined by the unitarization are shown in Figs. 1 and 2 and can be seen to be very close to the elastic solution below the first inelastic threshold at 773 MeV. In Figs. 3–5, we display the $K$-$\pi$ phase shifts. The phase shift $\delta_0{}^{1/2}$ in Fig. 3 resonates at about 887 MeV close to the $K^*$ resonance in the $\delta_1{}^{1/2}$ phase shift in Fig. 4. The resonance in the $\delta_0{}^{1/2}$ phase shift at 887 MeV is narrow with a width $\Gamma_{K^*}=60$ MeV measured between 45° and 135° in the phase shift. We show the world data for the $K$-$\pi$ phase shifts including the new data obtained by the Johns Hopkins group.[6] The

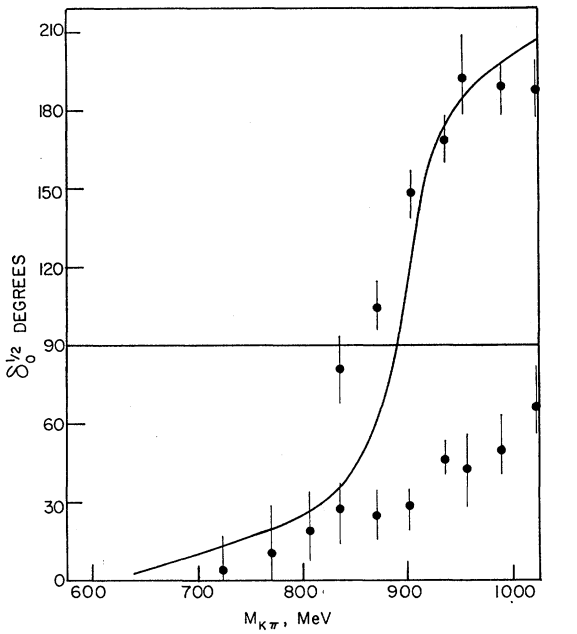


FIG. 3. Phase shift $\delta_{l=0}{}^{I=1/2}$ as a function of the $K\pi$ mass. The data are from Mercer *et al.* (Ref. 6). The down-up solution appears to be excluded by these data (see text.)

[6] T. G. Trippe *et al.*, Phys. Letters **28B**, 203 (1968); R. Mercer *et al.*, Johns Hopkins University report, 1970 (unpublished); and private communication.

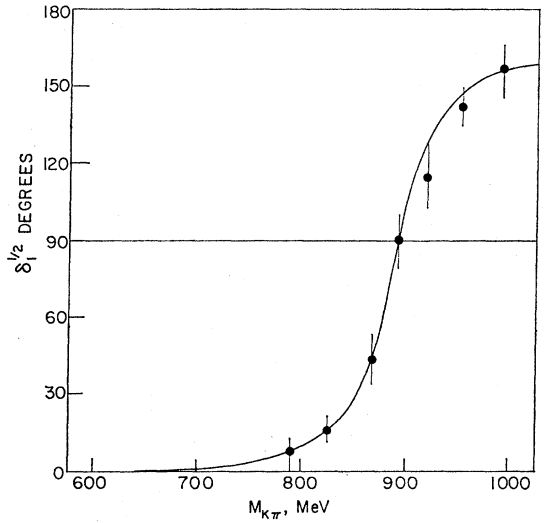


FIG. 4. Phase shift $\delta_{l=1}{}^{I=1/2}$. The data are from Mercer *et al.* (Ref. 6).

present experimental situation is that the down solution to $\delta_0{}^{1/2}$ in $K$-$\pi$ scattering does not cross over to the up solution around 890 MeV. However, our phase shift follows the down solution below the $K^*$ and the up solution above the $K^*$, and it may be that future experiments will allow a down-up solution. The fit to the $\delta_1{}^{1/2}$ phase-shift data is very good. The $\delta_0{}^{3/2}$ phase-shift data has large errors and our solution is consistent with the data. The $K^*$ resonance in the $\delta_1{}^{1/2}$ phase shift at 892 MeV has approximately the correct width $\Gamma_{K^*}=57$ MeV compared to the experimental width $(\Gamma_{K^*})_{\text{exp}}=50.1\pm0.8$ MeV.[7]

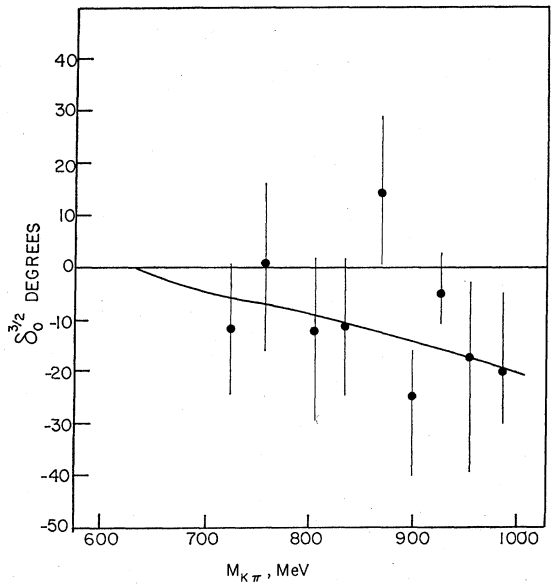


FIG. 5. Phase shift $\delta_{l=0}{}^{I=3/2}$. The data are from Mercer *et al.* (Ref. 6).

[7] Particle Data Group, Rev. Mod. Phys. **41**, 1 (1969).

It should be mentioned at this junction that because we unitarize the model by adding an imaginary part to the $\rho$ and $K^*$ trajectories, the total widths of all resonances will be equal at the positions of the poles in the second sheet. However, because of appreciable background effects due to the Pomeranchukon and the nonresonant scattering, the widths obtained directly from the predicted phase shifts and cross sections are not the same for all the resonances. They correspond to the physical widths which should be compared with the data. In this sense, a narrow-resonance approximation can be very misleading and, in fact, incorrect, since it completely ignores the large background scattering. We touch upon this question further in our discussion of the $\pi$-$\pi$ scattering results.

The charged states $K^+\pi^-\to K^+\pi^-$ and $K^+\pi^-\to K^0\pi^0$ correspond to the isospin combinations

$$\begin{aligned}\{K^+\pi^-\to K^+\pi^-\}&=\tfrac{2}{3}A^{1/2}+\tfrac{1}{3}A^{3/2},\\ \{K^+\pi^-\to K^0\pi^0\}&=\tfrac{1}{3}\sqrt{2}(-A^{1/2}+A^{3/2}).\end{aligned}\tag{4.5}$$

The total cross sections calculated from the model for these processes are shown in Figs. 6 and 7, and comparisons with the Veneziano-Lovelace[8] results based on the $K$ matrix are also shown. Our fits to the data are better than the Veneziano-Lovelace fits, particularly at

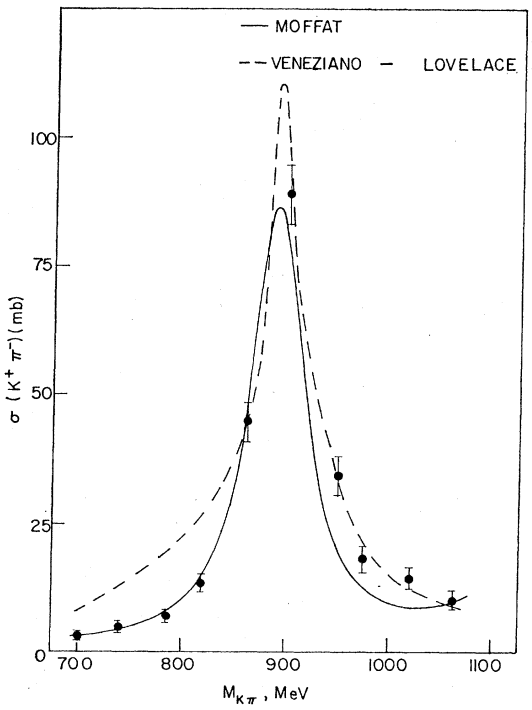


FIG. 6. Elastic cross section $\sigma(K^+\pi^-)$ as a function of the $K\pi$ mass. The data are from Trippe *et al.* (Ref. 6). The solid line is our fit; the dashed line is Lovelace's $K$-matrix Veneziano model (Ref. 8).

[8] C. Lovelace, in Proceedings of the ANL Conference on $\pi$-$\pi$ and $K$-$\pi$ Interactions, 1969, p. 562 (unpublished).

low energies and at the peaks of the cross sections determined by unitarity.

The $S$-wave scattering lengths are predicted to be

$$a_{1/2}=0.15m_\pi^{-1},$$
$$a_{3/2}=-0.06m_\pi^{-1}, \tag{4.6}$$

which are close to the current-algebra predictions[9]

$$a_{1/2}=(0.13\pm0.02)m_\pi^{-1},$$
$$a_{3/2}=-(0.07\pm0.01)m_\pi^{-1}, \tag{4.7}$$

determined in terms of the experimental pion decay constant $f_\pi=(1.03\pm0.05)m_{\pi^+}^{-1}$.

## V. RESULTS FOR $\pi$-$\pi$ SCATTERING ON THE MASS SHELL

We now consider the results obtained for low-energy $\pi$-$\pi$ scattering. All the parameters determined by the $K$-$\pi$ unitarization at low energies are used to predict the low-energy $\pi$-$\pi$ scattering with the exception of a change in the coupling constant $\gamma$. We therefore predict the low-energy $\pi$-$\pi$ scattering in terms of an effectively zero-parameter model, since the over-all normalization constant $\gamma$, determined for $\pi$-$\pi$ scattering to be $\gamma=167$, corresponds to $\gamma_{\rho\pi\pi}{}^2/4\pi=2.4$. This value is in agreement with Sakurai's[10] determination of $\gamma_{\rho\pi\pi}{}^2/4\pi$, which has an error of about 20%. The Adler condition determines the Pomeranchukon subtraction constant $D$ to be $-2.64\times10^{-4}$.

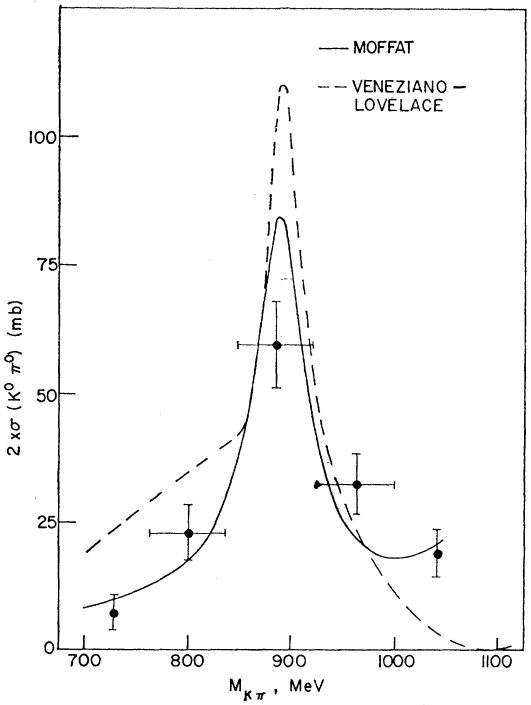


FIG. 7. Same as Fig. 6 for the charge-exchange cross section $2\times\sigma(K^+\pi^-\to K^0\pi^0)$.

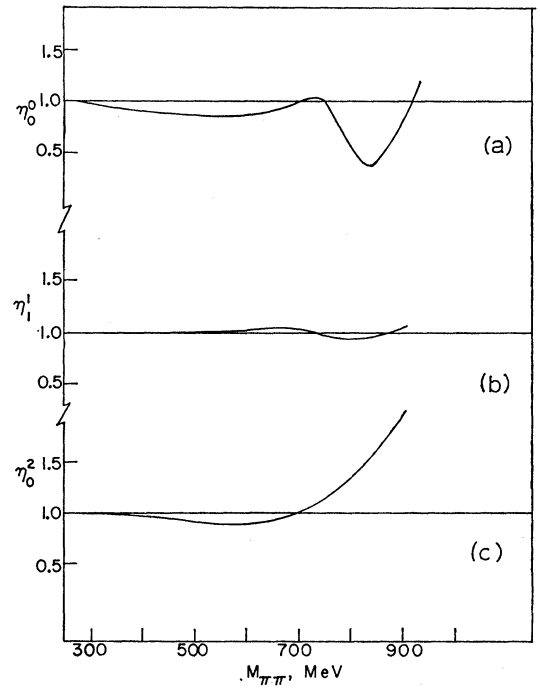


FIG. 8. Absorption parameter $\eta_l{}^I$ predicted for $\pi\pi$ scattering as a function of the $\pi\pi$ mass. (a) $\eta_{l=0}{}^{I=0}$. (b) $\eta_{l=1}{}^{I=1}$. (c) $\eta_{l=0}{}^{I=2}$.

Figure 8 shows the predicted results for the absorption parameters $\eta_0{}^0$, $\eta_1{}^1$, and $\eta_0{}^2$. The violation of elastic unitarity between 280 and 560 MeV is less than 10% in the $I=0$ $S$ wave and is negligible in the $I=1$ and $I=2$ waves. However, unitarity begins to be violated above $\approx$900 MeV, particularly in the $I=2$ $S$ wave. Thus, we can believe the phase shifts up to about 900 MeV, since small violations of unitarity were found to produce only an error of 1 or 2 degrees in the phase shifts. However, the cross sections are sensitive to $\eta$ and violations of unitarity may be expected to show up there (see Table I for the parameters used).

Figure 9 shows the $I=0$ $S$-wave phase shift as compared with the data of Cline *et al.*, Walker *et al.*, Biswas *et al.*, and Malamud and Schlein[11]; the latter do not include $I=2$ scattering, so their results are not fully consistent. We predict a resonant solution, of mass and width

$$m_\epsilon=725\text{ MeV},\quad \Gamma_\epsilon=194\text{ MeV}, \tag{5.1}$$

corresponding to a fairly broad $\epsilon$ resonance. The contribution of the Pomeranchukon to the $I=0$ phase shift is important, and causes a shift in the $\epsilon$ mass and a large broadening of the peak; this results in a broad

[9] J. A. Cronin, Phys. Rev. 161, 1483 (1967).
[10] J. J. Sakurai, Phys. Rev. Letters 17, 1021 (1966).
[11] D. Cline, K. J. Braun, and V. R. Scherer, University of Wisconsin report, 1969 (unpublished); W. Walker *et al.*, Phys. Rev. Letters 18, 630 (1967); N. Biswas *et al.*, Phys. Letters 27B, 513 (1968); E. Malamud and P. E. Schlein, Phys. Rev. Letters 19, 1056 (1967).

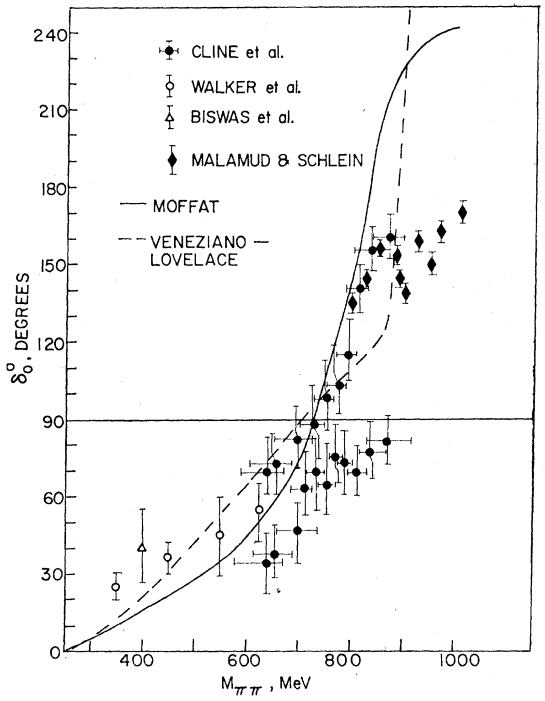


FIG. 9. Phase shift $\delta_{l=0}{}^{I=0}$ with the data of Cline *et al.*, Walker *et al.*, Biswas *et al.*, and Malamud and Schlein (Ref. 11). The dashed line is Lovelace's $K$-matrix Veneziano solution (Ref. 8); the solid line is our fit.

resonance near the $\rho$, as would be seen experimentally. We have also plotted Lovelace's solution,[8] which gives a broader resonance ($\Gamma_\epsilon=360$ MeV) at the same mass. His solution, however, results from a coupled-channel approach ($\pi\pi\to K\bar{K},\pi\pi$) using the $K$ matrix, which violates crossing symmetry.

Figure 10 shows the predicted $I=2$ $S$-wave phase shift, together with Lovelace's result. The data are from Baton *et al.*,[12] Katz *et al.*,[13] and Walker *et al.*[11] Up to 600 MeV, our solution is quite good; at higher energies, however, it falls below the data points. At $M_{\pi\pi}=500$ MeV, we predict

$$\delta_0{}^2(m_K)=-12^\circ, \tag{5.2}$$

giving

$$\delta_0{}^0(m_K)-\delta_0{}^2(m_K)=+39^\circ,$$

which is consistent with the results obtained from $K_L{}^0\to 2\pi^0$.[14] Morgan and Shaw[15] predict on the basis of a dispersion-relation calculation the results

$$\delta_0{}^0(m_K)=(33\pm 5)^\circ, \tag{5.3}$$

which compares favorably with our value $\delta_0{}^0(m_K)=27^\circ$.

[12] J. P. Baton, G. Laurens, and J. Reignier, Nucl. Phys. **B3**' 349 (1967).
[13] W. M. Katz *et al.*, in Proceedings of the ANL Conference on $\pi$-$\pi$ and $K$-$\pi$ Interactions, 1969, p. 300 (unpublished).
[14] G. E. Kalmus, in Proceedings of the ANL Conference on $\pi$-$\pi$ and $K$-$\pi$ Interactions, 1969, p. 413 (unpublished).
[15] D. Morgan and G. Shaw, Phys. Rev. D **2**, 520 (1970).

Lovelace[8] gets

$$\delta_0{}^0(m_K)=43^\circ \tag{5.4}$$

and

$$\delta_0{}^0(m_K)-\delta_0{}^2(m_K)=+55^\circ. \tag{5.5}$$

Figure 11 shows the $I=1$, $P$-wave phase shift, the usual $\rho$ Breit-Wigner solution.

Our $D$, $F$, and higher waves are quite small; the $D$ wave is about 1 or 2 degrees at the $\rho$ mass and there are no observable effects due to high-spin ancestors in the higher waves (see Table V).

At threshold, we predict for the $\pi$-$\pi$ scattering lengths

$$\begin{aligned} a_0&=0.19m_\pi{}^{-1},\\ a_1&=0.036m_\pi{}^{-3},\\ a_2&=-0.046m_\pi{}^{-1}, \end{aligned} \tag{5.6}$$

with

$$a_0/a_2=-4.1. \tag{5.7}$$

These results are close to the current-algebra values of Weinberg[3] and the predictions of chiral $SU(2)\otimes SU(2)$ which gives[9]

$$\begin{aligned} a_0&=(0.15\pm 0.02)m_\pi{}^{-1},\\ a_2&=-(0.04\pm 0.004)m_\pi{}^{-1}, \end{aligned} \tag{5.8}$$

using the pion decay constant $f_\pi=(1.03\pm 0.05)m_\pi{}^{+-1}$. They are also consistent with the experimental value for $a_0/a_2$ given by

$$a_0/a_2=-3.2\pm 1.0, \tag{5.9}$$

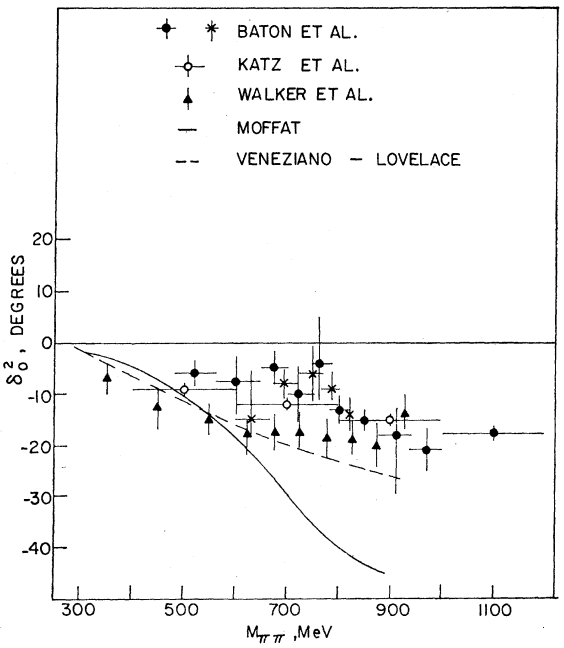


FIG. 10. Phase shift $\delta_{l=0}{}^{I=2}$ with the data points of Baton *et al.* (Ref. 12), Katz *et al.* (Ref. 13), and Walker *et al.* (Ref. 11). The solid line is our fit; the dashed line is Lovelace's fit (Ref. 8).

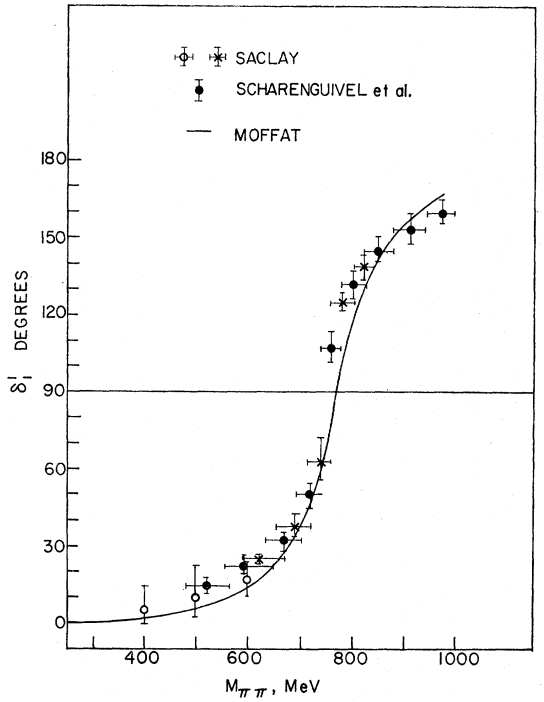


FIG. 11. Phase shift $\delta_{l=1}{}^{I=1}$ with the data of Saclay (Ref. 12) and Scharenguivel *et al.* (Ref. 23). The solid line is our fit.

obtained from the $\pi^+\pi^-$ asymmetry[16] and from the branching ratios[17]

$$\frac{\sigma(\pi^+\pi^-\to\pi^0\pi^0)}{\sigma(\pi^+\pi^+\to\pi^+\pi^+)} \quad\text{and}\quad \frac{\sigma(\pi^+\pi^-\to\pi^0\pi^0)}{\sigma(\pi^+\pi^-\to\pi^+\pi^-)} \tag{5.10}$$

near threshold. The solutions of Morgan and Shaw[15] give

$$\begin{aligned} a_0&=(0.16\pm0.04)m_\pi{}^{-1},\\ a_2&=-(0.05\pm0.01)m_\pi{}^{-1} \end{aligned} \tag{5.11}$$

for all reasonable input forms for the phase-shift solution. These scattering lengths are consistent with our results (Table II).

TABLE II. Predicted scattering lengths ($m_\pi{}^{-1}$).

| | | | |
|---|---|---|---|
| $\pi\pi$ | $a_0=0.19$, | $a_1=0.036m_\pi{}^{-2}$, | $a_2=-0.046$ |
| $K\pi$ | $a_{1/2}=0.15$, | $a_{3/2}=-0.06$ | |

The other quantity of importance is

$$L=\tfrac{1}{6}(2a_0-5a_2), \tag{5.12}$$

which can be evaluated by assuming that the $\pi$-$\pi$ $t$-channel $I=1$ amplitude satisfies an unsubtracted dispersion relation. This gives[5]

$$L=\frac{m_\pi{}^2}{6\pi}\int_{2m_\pi}^{\infty}\frac{d\nu}{(\nu^2-4m_\pi{}^2)}[2A_0{}^0(\nu,0) -5A_0{}^2(\nu,0)+3A_1{}^1(\nu,0)], \tag{5.13}$$

where $\nu=(s-u)/2m_\pi$. In Table III, we summarize the results of several current-algebra and model evaluations[18] of $L$. The poorness of Lovelace's scattering-length predictions is due to the violation of crossing symmetry which the $K$-matrix method gives.

We also satisfy approximately the result [partial conservation of axial-vector current (PCAC) and linearity][3]

$$2a_0-5a_2=18m_\pi{}^2a_1. \tag{5.14}$$

The left-hand side gives 0.618 and the right-hand side gives 0.653.

Our $P$-wave scattering length $a_1=0.036m_\pi{}^{-3}$ agrees with the Morgan and Shaw[15] calculation

$$a_1=(0.035\pm0.002)m_\pi{}^{-3} \tag{5.15}$$

and also with the result

$$a_1=(0.04\pm0.005)m_\pi{}^{-3} \tag{5.16}$$

quoted by Olsson.[19]

TABLE III. Comparison of results of several evaluations of $L$.

| Source | $L$ | $\alpha_0/\alpha_2$ | Remarks |
|---|---|---|---|
| Adler (Ref. 5), Weinberg (Ref. 3) | 0.10±0.01 | −3.5 | Amplitude linear about Adler point; PCAC |
| Tryon (Ref. 18) | 0.11±0.01 | −3.5 | "Unitary, crossing-symmetric numerical procedure" |
| Morgan and Shaw (Ref. 15) | 0.10±0.01 | −3.2±1.0 | "Unique solution to $\pi\pi$ scattering"—numerical unitarization of fixed-$t$ dispersion relations |
| Lovelace (Ref. 8) | 0.15 | −4.5 | "$K$ matrix" on Veneziano coupled channel. |
| Morgan and Shaw (Ref. 15) (Lovelace III) | 0.11 | −14.5 | As above, with Lovelace's phase shifts |
| J. Cronin (Ref. 9) | 0.09±0.01 | −3.7±0.8 | Chiral Lagrangian model |
| This model | 0.10 | −4.1 | Evaluated from scattering lengths |

[16] L. J. Gutay, F. T. Meire, and J. H. Scharenguivel, Phys. Rev. Letters **23**, 431 (1969).
[17] D. Cline, K. J. Braun, and V. R. Scherer, in Proceedings of the ANL Conference on $\pi$-$\pi$ and $K$-$\pi$ Interactions, 1969, p. 179 (unpublished).
[18] E. P. Tryon, in Proceedings of the ANL Conference on $\pi$-$\pi$ and $K$-$\pi$ Interactions, 1969, p. 665 (unpublished). See also J. B. Carrotte and R. C. Johnson, Phys. Rev. D **2**, 1945 (1970).
[19] M. G. Olsson, Phys. Rev. **162**, 1338 (1967).

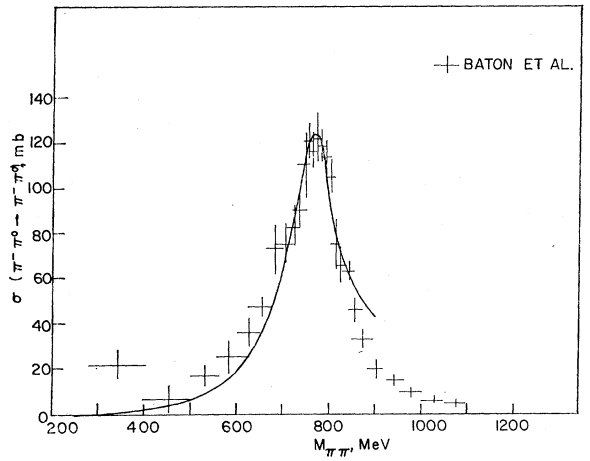


FIG. 12. Elastic cross section for $\pi^-\pi^0$, plotted against the $\pi\pi$ mass. The data are from Baton *et al.* (Ref. 12). The solid line is our fit.

The on-mass-shell elastic cross sections and charge-exchange cross sections are calculated using (2.10) and

$$\sigma = 16\pi \sum_l (2l+1)|f_l(s)|^2. \tag{5.17}$$

We must divide $\sigma$ by 2 in the case of identical particles (e.g., $\pi^+\pi^+ \to \pi^+\pi^+$ and $\pi^0\pi^0 \to \pi^0\pi^0$ scattering). Figure 12 shows the cross section for $\pi^-\pi^0$ elastic scattering compared with the data obtained by Baton *et al.*[12] in terms of a Chew-Low extrapolation of $d^2\sigma/d\Delta^2 ds$ for $\pi^- n \to \pi^-\pi^0 n$ to the pion pole. The fit is quite good, except above 900 MeV, where we begin to violate unitarity in the $I=1$ and $I=2$ waves; we reach the unitarity limit at 765 MeV, as we should. The $\pi^+\pi^-$ elastic-cross-section prediction is shown in Fig. 13 compared with the data of Johnson *et al.*[20] The number of data points is not impressive, but we fit the few that there are well enough. In Fig. 14, we display our

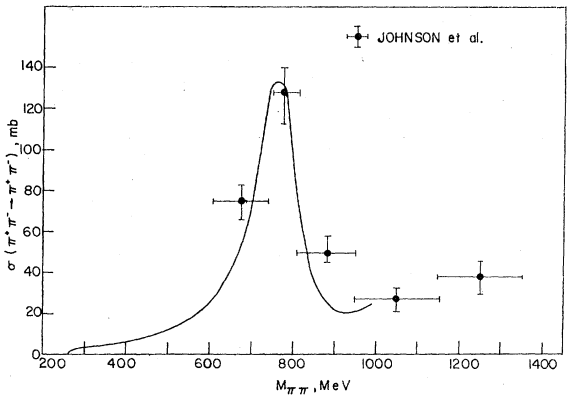


FIG. 13. Elastic cross section for $\pi^+\pi^-$ and our fit. Data from Johnson *et al.* (Ref. 20).

[20] P. B. Johnson *et al.*, Phys. Rev. **176**, 1651 (1968).

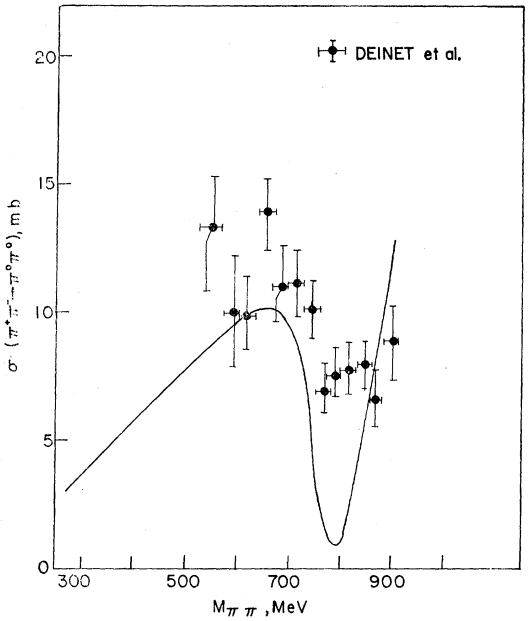


FIG. 14. Charge-exchange cross section $\sigma(\pi^+\pi^- \to \pi^0\pi^0)$ with data from Deinet *et al.* (Ref. 21). The solid line is our fit.

predicted charge-exchange cross section for $\pi^+\pi^- \to \pi^0\pi^0$ and compare it to the data of Deinet *et al.*[21] The agreement does not seem very impressive at first sight.

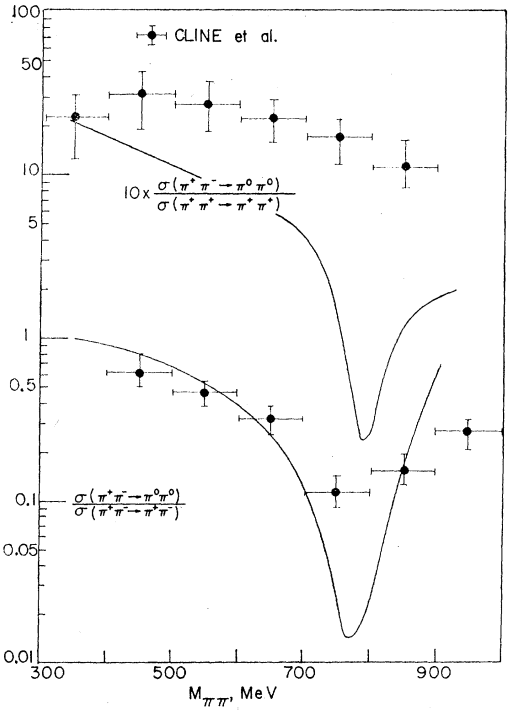


FIG. 15. Summary of Figs. 13 and 14: We plot the data of Cline *et al.* (Ref. 17) for the ratios $10\times\sigma(\pi^+\pi^- \to \pi^0\pi^0)/\sigma(\pi^+\pi^+ \to \pi^+\pi^+)$, $\sigma(\pi^+\pi^- \to \pi^0\pi^0)/\sigma(\pi^+\pi^- \to \pi^+\pi^-)$ with our fits.

[21] W. Deinet *et al.*, Phys. Letters **30B**, 359 (1969).

However, most experiments have been done at too low a beam energy with few events and lack of statistics. The competing $N^*$ formation causes problems, and since different experiments quote varying fractions of $N^*$'s, violently different cross sections are quoted by different groups because of the smallness of the absolute cross section. Morgan and Shaw[15] use the experimental points in Fig. 14 as evidence for a broad $I=0$ $S$ wave, not resonating until 900 MeV or higher (between-down solutions I and II). If this interpretation is correct, then no model with an $\epsilon$ daughter of the $\rho$ can fit the data. The phase shift has to remain around 90° to reproduce the data in Fig. 14, but in our model it rises through 180° rapidly giving the dip at 800 MeV. In fact, our fit has the typical broad resonance shape, as we should expect.

Much the same remarks apply to Fig. 15, which shows the ratios of cross sections

$$R_1=\sigma(\pi^+\pi^-\to\pi^0\pi^0)/\sigma(\pi^+\pi^+\to\pi^+\pi^+),$$
$$R_2=\sigma(\pi^+\pi^-\to\pi^0\pi^0)/\sigma(\pi^+\pi^-\to\pi^+\pi^-). \tag{5.18}$$

The dip we find in the charge-exchange cross section is, of course, faithfully reproduced in Fig. 15. The data dip in $R_2$ because the $\sigma(\pi^+\pi^-\to\pi^+\pi^-)$ is resonating; in $R_1$, $\sigma(\pi^+\pi^+)$ is not, so there is no dip. Morgan and Shaw conclude that $\delta_0{}^2(m_\rho)=-15°$ is favored from $R_1$. We get $\delta_0{}^2(m_\rho)=-27°$ and hence fall below the data points (data from Cline *et al.*[17]).

The asymmetry parameter is defined by[22]

$$\frac{F-B}{F+B}=\int_0^1 d\cos\theta\left[\frac{d\sigma(\cos\theta)}{d\Omega}-\frac{d\sigma(-\cos\theta)}{d\Omega}\right]\Big/\sigma_T, \tag{5.19}$$

where $\sigma_T$ denotes the total cross section. By using

$$d\sigma/d\Omega=|f^I(s,\cos\theta)|^2$$
$$=|2\sum_l(2l+1)P_l(\cos\theta)f_l{}^I(\cos\theta)|^2, \tag{5.20}$$

we get

$$\frac{F-B}{F+B}=4\sum_l\sum_{l'}(2l+1)(2l'+1)f_l(s)f_{l'}{}^*(s)$$
$$\times\int_0^1 dx[P_l(x)P_{l'}(x)-P_l(-x)P_{l'}(-x)]. \tag{5.21}$$

Next we substitute for one of the $P_{l'}$'s in terms of

$$P_{l'}(x)=\sum_{\lambda=0}^{[\frac{1}{2}l']}\frac{(-1)^\lambda(2l'-2\lambda)!x^{l'-2\lambda}}{2^{l'}\lambda!(l'-\lambda)!(l'-2\lambda)!}, \tag{5.22}$$

where $[\frac{1}{2}l']$ is the largest integer $\leqslant\frac{1}{2}l$, and we use the integration formula

$$\int_0^1 P_l(x)x^{l'-2\lambda}dx$$
$$=\frac{(\sqrt{\pi})2^{-l'+2\lambda-1}(1+l'-2\lambda)!}{\Gamma(1+\frac{1}{2}l'-\lambda-\frac{1}{2}l)\Gamma(\frac{1}{2}l'-\lambda+\frac{1}{2}l+\frac{3}{2})}. \tag{5.23}$$

Then with

$$a_{ll'}=\sum_{\lambda=0}^{[\frac{1}{2}l']}\frac{[(-1)^\lambda+(-1)^{l+l'+\lambda+1}](2l'-2\lambda)!(\sqrt{\pi})2^{2\lambda-2l'-1}(l'+1-2\lambda)}{\lambda!(l'-\lambda)!\Gamma(\frac{1}{2}l'-\frac{1}{2}l-\lambda+1)\Gamma(\frac{1}{2}l'+\frac{1}{2}l-\lambda+\frac{3}{2})}, \tag{5.24}$$

this gives

$$\frac{F-B}{F+B}=4\sum_l\sum_{l'}(2l+1)(2l'+1)f_l(s)f_{l'}{}^*(s)a_{ll'}/\sigma_T. \tag{5.25}$$

For $l=l'$, this is zero; also it is symmetric in $l$ and $l'$. Thus,

$$\frac{F-B}{F+B}=8\sum_{l'<l}\frac{(2l+1)(2l'+1)\,\mathrm{Re}[f_l(s)f_{l'}{}^*(s)]}{16\pi\sum_{l''}(2l''+1)|f_{l''}(s)|^2}a_{ll'}. \tag{5.26}$$

If we integrate over the azimuthal angle and neglect $D$ and higher waves, we get

$$\frac{F-B}{F+B}=\frac{3\,\mathrm{Re}[f_1(s)f_0{}^*(s)]}{|f_0(s)|^2+3|f_1(s)|^2}. \tag{5.27}$$

Figure 16 gives the on-mass-shell asymmetry parameter for $\pi^+\pi^-$ as a function of $M_{\pi\pi}$. The data of Scharenguivel *et al.* are shown for comparison.[23] This prediction acts as a check on the phase shifts, especially $\delta_0{}^0$. We observe that our fit is very good. Also plotted are the fits of Arnowitt[24] and Wagner.[22]

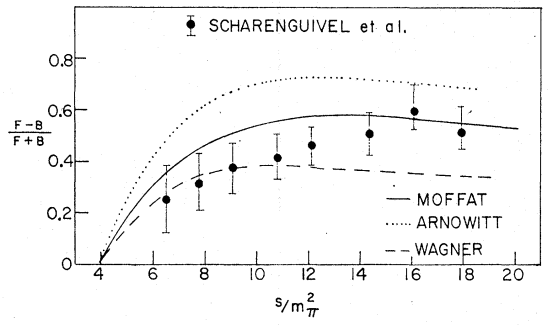


FIG. 16. On-mass-shell asymmetry parameter $(F-B)/(F+B)$ as a function of the $\pi\pi$ mass. Data from Scharenguivel *et al.* (Ref. 23). The solid line is our fit; the dashed line is Wagner's single-channel Veneziano ($K$-matrix) model (Ref. 22); the dotted line is a hard-pion current-algebra model due to Arnowitt (Ref. 24).

[22] F. Wagner, Nuovo Cimento 64A, 189 (1969).
[23] J. Scharenguivel *et al.*, Purdue University report, 1970 (unpublished).
[24] R. Arnowitt, in Proceedings of the ANL Conference on $\pi$-$\pi$ and $K$-$\pi$ Interactions, 1969, p. 619 (unpublished).

## VI. POSITIVITY AND CROSSING-SYMMETRY CONDITIONS BELOW THRESHOLD

General conditions on the $\pi$-$\pi$ scattering amplitude for the process $\pi^0\pi^0 \to \pi^0\pi^0$ below threshold have been derived by Martin[25] and others[26] from crossing symmetry, unitarity, and the existence of a twice-subtracted dispersion relation for the amplitude. We should expect to satisfy all of these conditions, because the model satisfies the correct analyticity properties, is crossing symmetric, and satisfies approximate unitarity; however, these conditions are a useful consistency check on our amplitude.

Let us write

$$A_0(\pi^0\pi^0 \to \pi^0\pi^0) = f_0{}^{00}. \tag{6.1}$$

In Fig. 17, the $S$-wave amplitude (6.1) is plotted between $s=0$ and $s=4m_\pi{}^2$. We see that $f_0{}^{00}$ has a unique minimum between $s=1.29m_\pi{}^2$ and $s=1.7m_\pi{}^2$. In Table IV, we list several conditions on $f_0{}^{00}$, which show that these rigorous requirements are fulfilled by the model.

## VII. OFF-MASS-SHELL BEHAVIOR

We now discuss the behavior of the model when one of the pions is extrapolated off the mass shell in both $\pi$-$\pi$ and $K$-$\pi$ scattering. This enables us to pass into the physical region for the processes $\pi N \to \pi\pi N$ and $KN \to K\pi N$ assuming the validity of the one-pion-exchange (OPE) approximation (see Fig. 18). Our on-mass-shell comparisons with the data also assume the validity of OPE, since this is how the data are obtained.

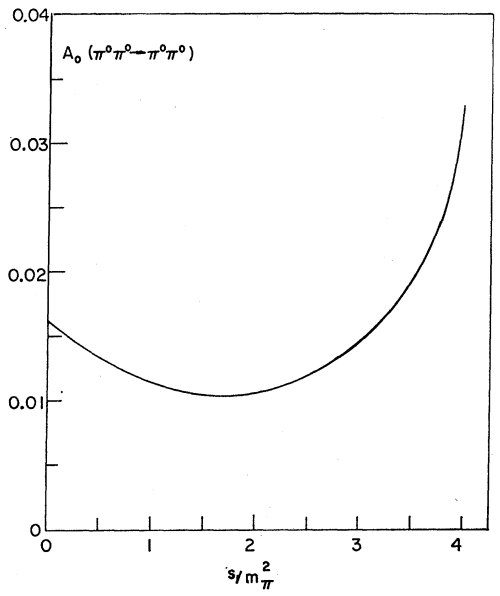


FIG. 17. $S$-wave amplitude for $\pi^0\pi^0 \to \pi^0\pi^0$ from $s=0$ to $s=4m_\pi{}^2$.

TABLE IV. Conditions (Refs. 25 and 26) on $A_0(\pi^0\pi^0 \to \pi^0\pi^0) \equiv f_0{}^{00}$ for $0 \leqslant s \leqslant 4(m_\pi=1)$.

| Condition | Satisfied | Remarks |
|---|---|---|
| (1) $f_0{}^{00}(s) < f_0{}^{00}(4)$ | yes | |
| (2) unique minimum in $f_0{}^{00}(s)$ between 1.29 and 1.7; i.e., $df_0{}^{00}(s)/ds<0$, $0\leqslant s\leqslant 1.29$ $df_0{}^{00}(s)/ds>0$, $1.7\leqslant s\leqslant 1.76$ | yes | minimum at 1.67 |
| (3) $df_0{}^{00}(s)/ds>0$, $2\leqslant s\leqslant 4$ | yes | |
| (4) $f_0{}^{00}(0) \geqslant f_0{}^{00}(2(1+1/\sqrt{3}))$ | yes | |
| (5) $d^2f^{00}(s)/ds^2>0$, $0\leqslant s\leqslant 1.7$ | yes | |
| (6) $f_0{}^{00\prime}(0) < -\frac{1}{4}[2f_0{}^{00}(4) - f_0{}^{00}(2) - f_0{}^{00}(0)]$ | yes | |
| (7) $f_0{}^{00}(0) \geqslant \frac{1}{2}\int_2^4 f_0{}^{00}(s)ds$ | yes | |

We assume that the off-mass-shell dependence of the amplitude is contained in the implicit dependence of $t$ and $u$ on the extrapolation, except for a possible form factor which is equal to unity on the mass shell.

Let us consider the $\pi N \to \pi\pi N$ system first. Our kinematical variables are defined in Fig. 18 and we follow the notation and derivation of Ferrari and Selleri.[27] For the $\pi\pi$ system, we have

$$\begin{aligned} s &= (q_1+k_3-q_2)^2 = (k_1+k_2)^2, \\ t &= (k_1-q_1)^2, \\ u &= (k_2-q_1)^2, \end{aligned} \tag{7.1}$$

and $q_1+q_2=k_1+k_2+k_3$. For the $\pi N$ system,

$$W^2 = (q_1+q_2)^2 = (k_1+k_2+k_3)^2. \tag{7.2}$$

We define $-\Delta^2$ as the (mass)$^2$ of the transferred pion, i.e., as the momentum transfer from the nucleon to the

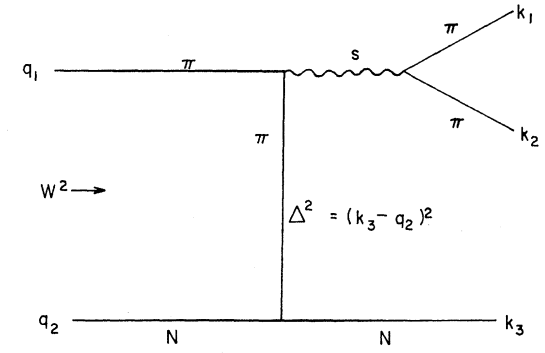


FIG. 18. Kinematical quantities used in the extrapolation of the exchanged pion off the mass shell. $q_1$, $q_2$ ($k_1$,$k_2$,$k_3$) are the incident (final) four-momenta; $W^2$ is the $\pi(q_1)N(q_2)$ c.m. energy squared; $s$ is the c.m. energy squared for the $2\pi \to 2\pi$ system. $-\Delta^2$ is the (mass)$^2$ of the exchanged pion.

[25] A. Martin, Nuovo Cimento **57A**, 393 (1967).

[26] A. K. Common, Nuovo Cimento **63A**, 482 (1968); O. Piguet and G. Wanders, Phys. Letters **30B**, 418 (1969); A. P. Balachandran and J. Nuyts, Phys. Rev. **172**, 1821 (1968); A. P. Balachandran and M. L. Blackmon, Syracuse University Report No. NYO-3399-223, 1970 (unpublished). G. Auberson, G. Mahoux, O. Brander, and A. Martin, Nuovo Cimento **65A**, 743 (1970). R. Roskies, Phys. Rev. D **2**, 247 (1970).

[27] E. Ferrari and F. Selleri, Nuovo Cimento **24**, 453 (1962).

pion. Thus, $\Delta^2=-m_\pi^2$ corresponds to being on the mass shell and

$$\Delta^2=-(q_2-k_3)^2=-(k_1+k_2-q_1)^2. \tag{7.3}$$

Other quantities of interest are the pion laboratory momentum $p_{\rm lab}$ and $t$ and $u$ as functions of $\Delta^2$. These are given by

$$p_{\rm lab}{}^2=\left(\frac{W^2-m_N{}^2-m_\pi{}^2}{2m_N}\right)^2-m_\pi{}^2,$$
$$t=\tfrac{1}{2}(3m_\pi{}^2-s-\Delta^2)+2q_{\rm on}q_{\rm off}\cos\theta, \tag{7.4}$$
$$u=\tfrac{1}{2}(3m_\pi{}^2-s-\Delta^2)-2q_{\rm on}q_{\rm off}\cos\theta,$$

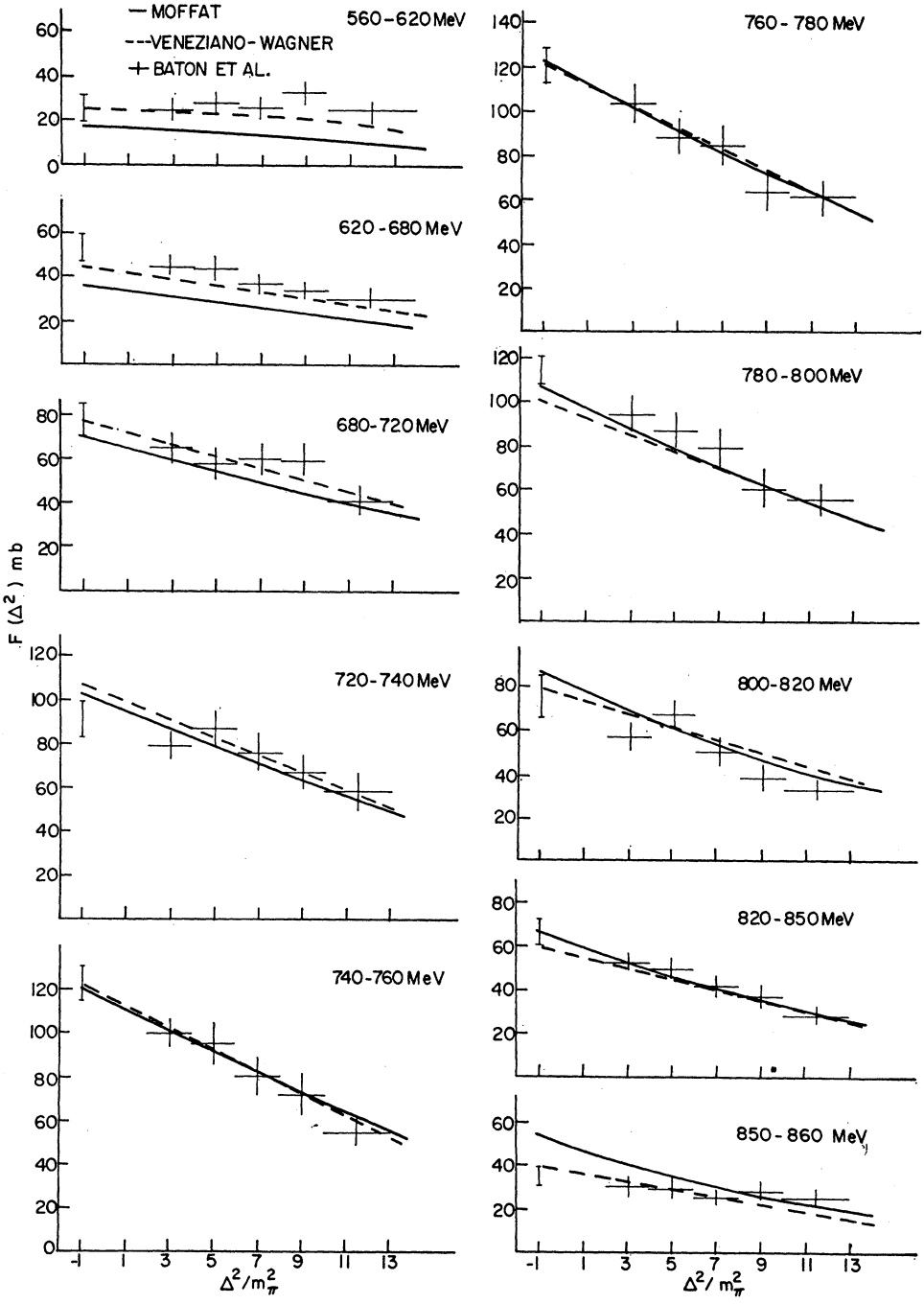


FIG. 19. Off-mass-shell extrapolations of the cross section for $\pi^-\pi^0\to\pi^-\pi^0$ as a function of $\Delta^2/m_\pi{}^2$. $F(\Delta^2,s)=(q_{\rm off}/q_{\rm on})\sigma_{\rm off}$. We have averaged $F$ over the energy region indicated in each graph. The data are from Baton *et al.* (Ref. 12). The dashed line is Wagner's (Ref. 22) fit; the solid line is ours.

where

$$q_{\rm on}^2=\tfrac{1}{4}s-m_\pi^2,$$
$$q_{\rm off}^2=[s^2+2(\Delta^2-m_\pi^2)s+(m_\pi^2+\Delta^2)^2]/4s. \quad (7.5)$$

We multiply the partial waves $f_l$ by the form factor $\exp[-\beta(\Delta^2+m_\pi^2)]$, where $\beta$ is a constant. Wagner[22] has justified the use of this phenomenological device as allowing for the Reggeization of the virtual pion setting

$$\beta=\alpha_\pi' \ln(W^2/W_0^2) \quad (7.6)$$

so that the form factor has the form

$$(W^2/W_0^2)^{-\alpha_\pi'(\Delta^2+m_\pi^2)}. \quad (7.7)$$

However, we should expect from the slope of the pion trajectory that $W_0^2\approx 1$ GeV$^2$. But Wagner[22] uses $W_0^2=0.3$ GeV$^2$ and, therefore, makes this particular justification of the form factor suspect.

Following Ferrari and Selleri,[27] we extrapolate the formula for the elastic cross section:

$$\sigma(s,\Delta^2)=16\pi\sum_l (2l+1)\exp[-2\beta(\Delta^2+m_\pi^2)]\times|f_l(s,\Delta^2)|^2 \quad (7.8)$$

off the mass shell. The partial-wave amplitudes off the mass shell are defined by

$$f_l^I(s,\Delta^2)=\frac{1}{2}\int_{-1}^{1} d\cos\theta\, f^I(s,\Delta^2)P_l(\cos\theta). \quad (7.9)$$

We then average (7.8) over small regions of $s$, and compare the results with the Chew-Low extrapolation data of Baton *et al.*[12] Figure 19 displays the fits of the present model and also Wagner's fits using the Veneziano model. We used $\beta=2.8$ GeV$^{-2}$ in all our $\pi\pi$ fits, whereas Wagner uses $\beta$ as an adjustable parameter, changing it slightly from the Chew-Low extrapolation to the differential cross section. Both models fit the data quite well, although in view of the arbitrariness of the form factor employed in the fits the significance of the results is not entirely clear.

The differential cross section $d\sigma/d\Delta^2$ is the quantity measured in the reaction $\pi N\to\pi\pi N$; it is extrapolated to give the total cross sections. In terms of partial waves, it is calculated to be

$$\frac{d^2\sigma}{d\Delta^2 ds}=\frac{1}{8\pi}\left(\frac{G_{\pi N}^2}{m_N^2 p_{\rm lab}^2}\right)\frac{\Delta^2 s^{1/2}q_{\rm on}}{(\Delta^2+m_\pi^2)^2}\times\sum_{l=0}^{\infty}(2l+1)|f_l^I(s,\Delta^2)|^2\times\exp[-2\beta(\Delta^2+m_\pi^2)][1+(-1)^{l+I}]^2, \quad (7.10)$$

where $G_{\pi N}^2/4\pi$ is the $\pi N$ coupling constant. We then average this over the $\rho$ region and get $d\sigma/d\Delta^2$, which is plotted in Figs. 20 and 21, and compared with the data of Jacobs,[28] and Wagner's fit.[22] Again the fits are good.

[28] L. D. Jacobs, LRL Report No. UCRL 16877, 1966 (unpublished).

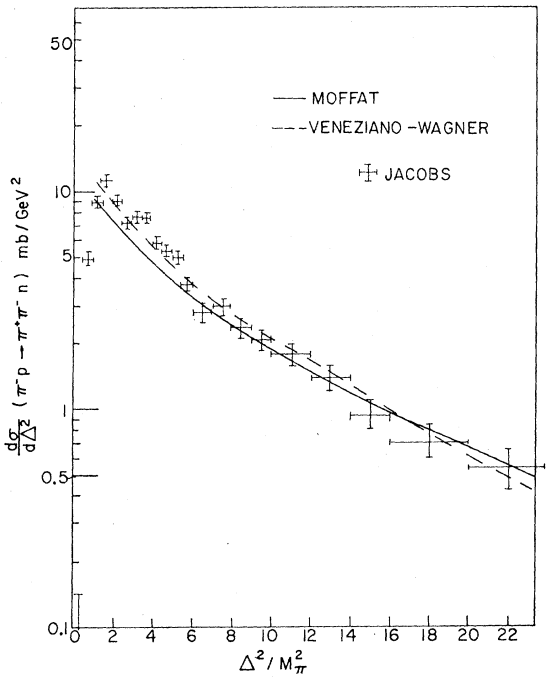


FIG. 20. Differential cross section $d\sigma/d\Delta^2$ for $\pi^- p\to\pi^+\pi^- n$, averaged over the $\rho$ region. The solid line is our fit; the dashed line is Wagner's (Ref. 22). The data are from Jacobs (Ref. 28).

However, in both our case and Wagner's calculations, the normalization is not quite correct. We must use $G_{\pi N}^2/4\pi=20$ instead of 15, and Wagner uses $G_{\pi N}^2/4\pi=15$ for one fit and $G_{\pi N}^2/4\pi=8.8$ for the other one.

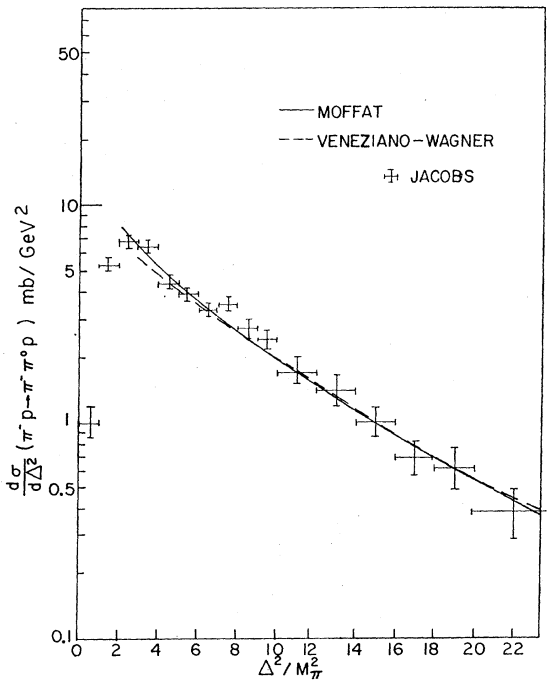


FIG. 21. Same as Fig. 20 for $\pi^- p\to\pi^-\pi^0 p$.

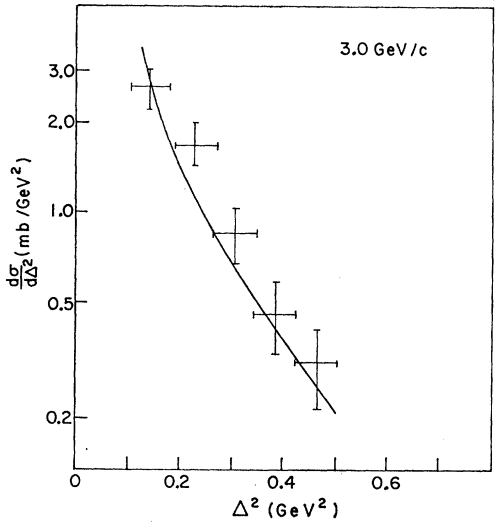


FIG. 22. Differential cross section $d\sigma/d\Delta^2$ for $K^+p \to K^*(890)\Delta^{++} \to K^+\pi^-\Delta^{++}$, averaged over the resonance. The data are from Trippe *et al.* (Ref. 6). The solid line is our fit. The kaon lab energy is $P_{\rm lab}=3.0$ GeV/$c$.

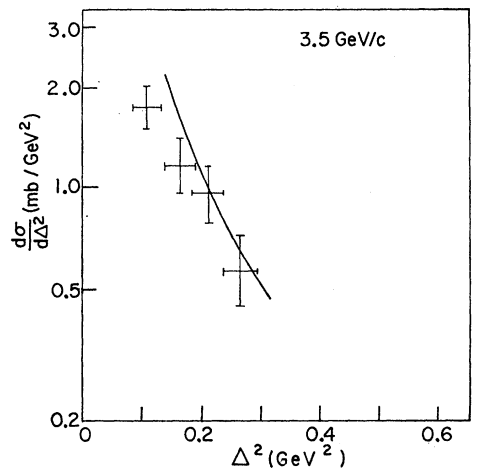


FIG. 23. Same as Fig. 22 for $P_{\rm lab}=3.5$ GeV/$c$.

Let us now consider the process $KN \to K\pi N$. We examine the cross section $d\sigma/d\Delta^2$ for the reaction $K^+p \to K^+\pi^-\Delta^{++}$ and assume, as before, that the reaction is dominated by the OPE mechanism. The momentum transferred to the kaon, squared, is denoted by $t$, and the c.m. energy squared in the $K^+\pi^-$ system is $s$. The coupling between the $p$, $\pi^-$, and $\Delta^{++}$ is assumed to be of the form

$$(G_{\pi\Delta}/M_\Delta)\bar{\psi}(x)\psi_\mu(x)\gamma^\mu\phi(x)+\text{H.c.} \qquad (7.11)$$

In the Ferrari-Selleri[27] formulation the quantity of interest is the summation over spin states of the expression

$$(q-p)^\mu(q-p)^\nu[\bar{u}(p)u(q)(\bar{u}_\nu(p)u_\mu(q))^\dagger], \qquad (7.12)$$

where $q^\mu$ and $p^\mu$ are the 4-momenta of the proton and the $\Delta^{++}$, respectively. Within an over-all constant factor, the spin summation of (7.12) gives

$$P=\frac{8}{3}\left(\frac{m_p^2+M_\Delta^2+\Delta^2}{2}\right)\Delta^2 + \frac{8}{3M_\Delta^2}\left(\frac{m_p^2+M_\Delta^2+\Delta^2}{2}+m_pM_\Delta\right)\times\left(\frac{M_\Delta^2-m_p^2-\Delta^2}{2}\right)^2. \qquad (7.13)$$

Then $d\sigma/d\Delta^2$ is given by

$$\frac{d\sigma}{d\Delta^2}=\left(\frac{G_{\pi\Delta}^2}{4\pi}\right)\frac{P\exp[-2\beta(\Delta^2+m_\pi^2)]^2}{(P_{\rm lab})^2(\Delta^2+m_\pi^2)^2} \times\left(\frac{4\pi}{m_p^2M_\Delta^2}\right)\int Q(\sqrt{s})\sum_l(2l+1)|f_l(s,\Delta^2)|^2ds. \qquad (7.14)$$

Here $Q$ is the c.m. 3-momentum in the $K$-$\pi$ system and $P_{\rm lab}$ is the magnitude of the incoming $K$ momentum in the $K$-$p$ lab system. The constant $\beta$ is chosen to be $\beta=3.8$ GeV$^{-2}$ and $G_{\pi\Delta}^2/4\pi$ is a dimensionless coupling constant $G_{\pi\Delta}^2/4\pi=0.44$.

The relation between $\Delta^2$ and $\cos\theta$ is

$$\cos\theta=\frac{s^2+s(2t-2m_K^2+\Delta^2-m_\pi^2)+(m_K^2+\Delta^2)(m_K^2-m_\pi^2)}{\lambda(s,m_K^2,-\Delta^2)\lambda(s,m_K^2,m_\pi^2)}, \qquad (7.15)$$

where

$$\lambda(x,y,z)=x^2+y^2+z^2-2xy-2xz-2yz. \qquad (7.16)$$

The off-mass-shell partial-wave amplitudes are found from (7.9), where the relationship between $\cos\theta$ and $\Delta^2$ is given by (7.15).

In Figs. 22–25, we show the predictions compared to the data of Trippe *et al.*[6] using $\beta=3.8$ GeV$^{-2}$, and we see that the fits are satisfactory.

## VIII. HIGH-ENERGY BEHAVIOR

In view of the success of the model in describing low-energy $\pi$-$\pi$ and $K$-$\pi$ scattering, it is interesting to study the $\pi$-$\pi$ and $K$-$\pi$ total cross sections and the $\pi$-$\pi$ differential cross sections at high energies.

Let us consider the asymptotic behavior of the $\pi$-$\pi$ amplitudes. The amplitude $F_\rho(s,t)$ has the following

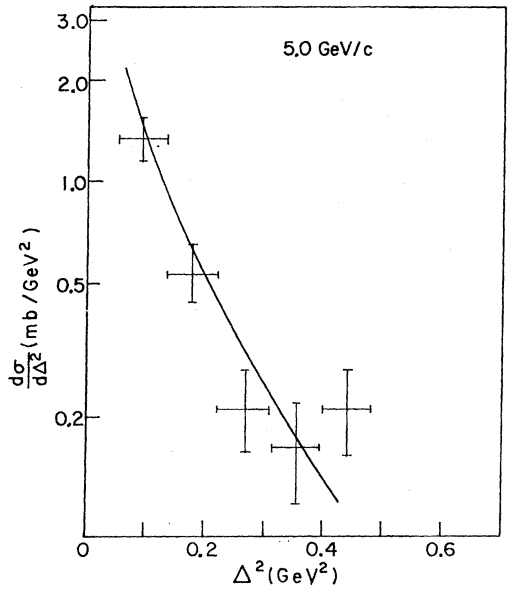


FIG. 24. Same as Fig. 22 for $P_{\text{lab}}=5$ GeV/$c$.

asymptotic behavior as $s\to\infty$ for fixed $t$ in the $s$ channel:

$$F_\rho(s,t)\sim -\frac{\pi\gamma_\rho(t)}{\Gamma(\alpha_\rho(t))}\frac{(-s/s_0)^{\alpha_\rho(t)}}{\sin\pi\alpha_\rho(t)},$$
$$F_\rho(t,u)\sim -\frac{\pi\gamma_\rho(t)}{\Gamma(\alpha_\rho(t))}\frac{(s/s_0)^{\alpha_\rho(t)}}{\sin\pi\alpha_\rho(t)}, \tag{8.1}$$
$$F_\rho(s,u)\to 0.$$

The Pomeranchukon amplitude has the asymptotic behavior in the $s$ channel for $s\to\infty$ and $t$ fixed:

$$P^I\sim A_P(t,s)+A_P(t,u)=\mathcal{P}(t,s). \tag{8.2}$$

This follows by virtue of the result that for $s\to\infty$ and $t$ fixed,

$$A_P(u,s)\approx A_P(u,t)\approx 0,$$
$$A_P(s,t)\approx A_P(s,u)\approx 0. \tag{8.3}$$

Therefore, the isospin amplitudes $f^I$ have the following asymptotic behavior in the $s$ channel for $s\to\infty$ and $t$ fixed:

$$f^{I=0}(s,\theta)\sim \frac{1}{16\sqrt{s}}\left[\frac{-\frac{1}{2}\gamma_\rho(t)}{\Gamma(\alpha_\rho(t))}\left(\frac{s}{s_0}\right)^{\alpha_\rho(t)}\times\frac{3e^{-i\pi\alpha_\rho(t)}-1}{\sin\pi\alpha_\rho(t)}+\mathcal{P}(t,s)\right],$$
$$f^{I=1}(s,\theta)\sim \frac{1}{16\sqrt{s}}\left[\frac{-\gamma_\rho(t)}{\Gamma(\alpha_\rho(t))}\left(\frac{s}{s_0}\right)^{\alpha_\rho(t)}\times\frac{e^{-i\pi\alpha_\rho(t)}}{\sin\pi\alpha_\rho(t)}+\mathcal{P}(t,s)\right], \tag{8.4}$$
$$f^{I=2}(s,\theta)\sim \frac{1}{16\sqrt{s}}\left[\frac{-\gamma_\rho(t)}{\Gamma(\alpha_\rho(t))}\left(\frac{s}{s_0}\right)^{\alpha_\rho(t)}\times\frac{1}{\sin\pi\alpha_\rho(t)}+\mathcal{P}(t,s)\right].$$

Since the term $\mathcal{P}(t,s)$ eventually dominates as $s$ increases, the amplitudes will become isospin-independent, as they should be.

The differential cross sections are given by

$$\frac{d\sigma}{dt}(\pi^+\pi^+)=\frac{\pi}{q^2}|f^{I=2}(s,\theta)|^2,$$
$$\frac{d\sigma}{dt}(\pi^+\pi^-)=\frac{\pi}{q^2}|\tfrac{1}{3}f^{I=0}(s,\theta)+\tfrac{1}{2}f^{I=1}(s,\theta)+\tfrac{1}{6}f^{I=2}(s,\theta)|^2,$$
$$\frac{d\sigma}{dt}(\pi^\pm\pi^0)=\frac{\pi}{q^2}|\tfrac{1}{2}f^{I=1}(s,\theta)+\tfrac{1}{2}f^{I=2}(s,\theta)|^2, \tag{8.5}$$
$$\frac{d\sigma}{dt}(\pi^0\pi^0)=\frac{\pi}{q^2}|\tfrac{1}{3}f^{I=0}(s,\theta)+\tfrac{2}{3}f^{I=2}(s,\theta)|^2,$$
$$\frac{d\sigma}{dt}(\pi^+\pi^-\to\pi^0\pi^0)=\frac{\pi}{q^2}|\tfrac{1}{3}[f^{I=2}(s,\theta)-f^{I=0}(s,\theta)]|^2.$$

By using the optical theorem, we can relate the total cross section to the imaginary part of the amplitude in the forward direction:

$$\sigma_T=\frac{4\pi}{q}\,\mathrm{Im}f^I(s,0). \tag{8.6}$$

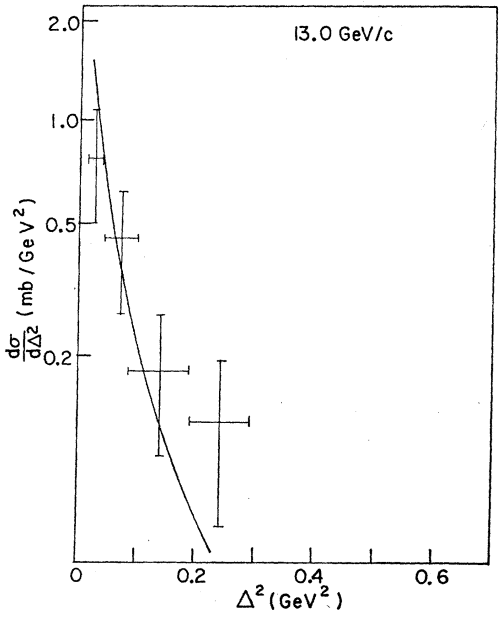


FIG. 25. Same as Fig. 22 for $P_{\text{lab}}=13$ GeV/$c$.

TABLE V. Predicted resonances.

| Name | $J^P$ | $I^G$ | Mass (MeV) Theory | Mass (MeV) Expt. | Decay mode | Partial width (MeV) Theory | Partial width (MeV) Expt. |
|---|---|---|---|---|---|---|---|
| $\epsilon$ | $0^+$ | $0^+$ | 725 | ~710 | $\pi\pi$ | 194 | 140–450 |
| $\rho$ | $1^-$ | $1^+$ | 765 | 765±10 | $\pi\pi$ | 120 | 125±20 |
| $f$ | $2^+$ | $0^+$ | 1285 | 1264±10 | $\pi\pi$ | 112[a] | $\lesssim$130 |
| $g$ | $3^-$ | $1^+$ | 1671 | 1650±20 | $\pi\pi$ | 18[a] | <120 |
| $K^*$ | $1^-$ | $\frac{1}{2}$ | 892 | 891.4±0.6 | $K\pi$ | 57 | 50.1±0.8 |
| $K'^*$ | $0^+$ | $\frac{1}{2}$ | 887 | ? | $K\pi$ | 60 | ··· |

[a] Calculated in the narrow-resonance approximation.

In Fig. 26, we show the differential cross section for charge-exchange scattering at several values of $s$. We observe that the ghost-eliminating zero in the residue at $t=-0.5$ causes a dip at this value of $t$, and there is also a dip near $t=0$ due to the zero in the residue at $t=m_\pi^2$. The dip at $t=-0.5$ becomes more pronounced as the energy increases because the signature factor becomes exact only at infinite energy. There is no zero at $t=-0.1$; this zero would be expected to occur if factorization were valid and the crossover in $\pi N$ scattering were caused by the vanishing of the non-spin-flip residue for the $\rho$ trajectory. The differential cross sections for the elastic $\pi$-$\pi$ processes are shown for $s=40$ and 80 GeV$^2$ in Fig. 27. These cross sections are structureless, as would be expected, due to the dominance of the Pomeranchukon amplitude at these energies.

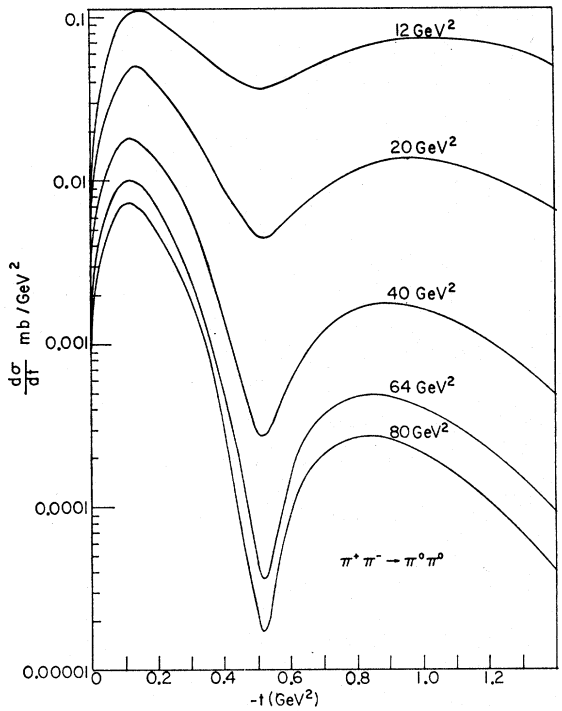


FIG. 26. Differential cross section $d\sigma/dt$ for $\pi^+\pi^- \to \pi^0\pi^0$ as a function of $t$, for $s=12$, 20, 40, 64, and 80 GeV$^2$.

Figure 28 shows the total cross sections for $\pi$-$\pi$ scattering at high energies. The asymptotic limit of the cross sections is $\approx 8$ mb for all charge states; this can be compared to the value of $\approx 13$ mb obtained from factorization using

$$\sigma_{\pi\pi}=\sigma_{\pi N}^2/\sigma_{NN} \tag{8.7}$$

and the presently available data.[29] The contribution from the $\rho$-Regge pole is determined by the result at $s=20$ GeV$^2$:

$$\sigma_{\pi^+\pi^-}-\sigma_{\pi^+\pi^+}=-0.5 \text{ mb}. \tag{8.8}$$

Because experimentally

$$\sigma_{\pi^- p}-\sigma_{\pi^+ p}=1.5 \text{ mb} \tag{8.9}$$

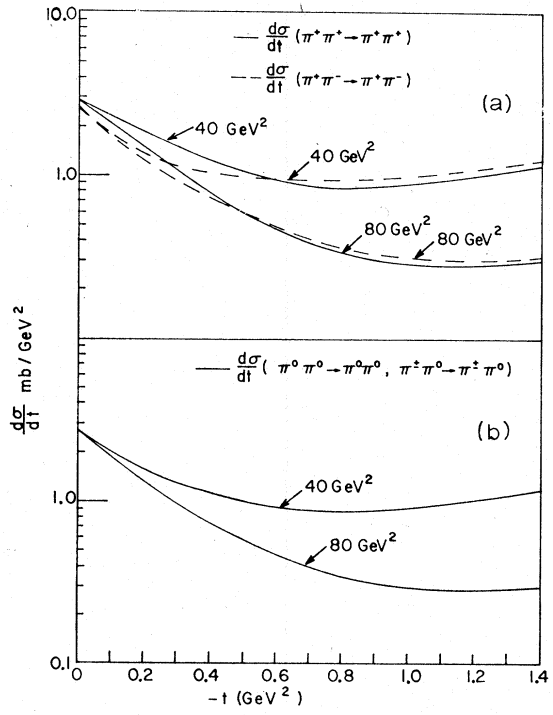


FIG. 27. (a) $d\sigma/dt$ for $\pi^+\pi^+ \to \pi^+\pi^+$ (solid line), $\pi^+\pi^- \to \pi^+\pi^-$ (dashed line) for $s=40$, 80 GeV$^2$. (b) $d\sigma/dt$ for $\pi^0\pi^0 \to \pi^0\pi^0$, $\pi^\pm\pi^0 \to \pi^\pm\pi^0$ for $s=40$, 80 GeV$^2$.

[29] S. V. Allaby *et al.*, Phys. Letters **30B**, 500 (1969).

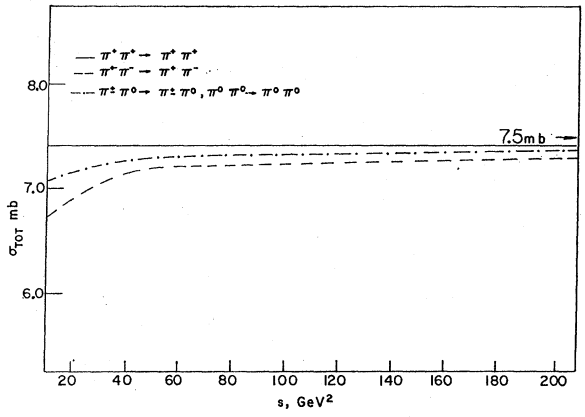


FIG. 28. Total cross section $\sigma_T$ for $\pi^+\pi^+$ (solid line), and the elastic cross sections for $\pi^+\pi^-$ (dashed line), and $\pi^0\pi^0$, $\pi^\pm\pi^0$ (dash-dot line) as a function of $s$.

at this energy has the opposite sign, we do not have strict factorization for the $\rho$ contribution, as we already observed in the $\pi$-$\pi$ charge-exchange scattering. The asymptotic $K$-$\pi$ total cross section is 4 mb, which can be compared with the value of $\approx 11$ mb obtained from factorization using

$$\sigma_{K\pi} = \sigma_{KN}\sigma_{\pi N}/\sigma_{NN} \tag{8.10}$$

and the presently available data.[29]

## IX. CONCLUSIONS

We have succeeded in finding solutions to the model for $K$-$\pi$ scattering which are approximately unitary at low energies and satisfy $s$-$u$ crossing exactly; the on-mass-shell predictions were in satisfactory agreement with the data, and the scattering lengths were close to those obtained from current algebra. Apart from a change in the over-all coupling constant, the same parameters were then used to predict the low-energy $\pi$-$\pi$ scattering and the crossing-symmetric solutions were found to be approximately unitary up to 900 MeV, and satisfactory fits to the available data (see Table V) were found except in the case of the charge-exchange data; however, the latter data are still open to question due to the difficulty in measuring the cross sections for this process accurately, and further experimental information is required. The predicted on-mass-shell forward-backward asymmetry fitted the data very well, and the predicted scattering lengths at threshold were in good agreement with various analyses of the data and the results of current algebra.

The general conditions below threshold that follow from crossing symmetry and positivity were investigated and found to be well satisfied. The calculation of the high-energy $\pi$-$\pi$ and $K$-$\pi$ scattering showed that the Pomeranchukon amplitude described the low- as well as the high-energy region satisfactorily; the charge-exchange scattering at high energy displayed the "nonsense" dip correctly, and the total cross sections were found to be of the order of magnitude expected in the asymptotic region.

If we could succeed in extending the model to the resonance region at intermediate energies by some satisfactory procedure of unitarization, then we could claim to have an approximate description of $\pi$-$\pi$ and $K$-$\pi$ scattering valid in the whole energy range, consistent with the basic principles that we believe a model of strong interactions should possess.

PHYSICAL REVIEW D VOLUME 3, NUMBER 5 1 MARCH 1971

# Contribution of Elastic Intermediate States to Polarization of the Recoil Proton in Elastic Electron-Proton Scattering

A. J. G. HEY*
*Department of Theoretical Physics, University of Oxford, Oxford, England*
(Received 9 November 1970)

The polarization of the recoil proton in the elastic scattering of unpolarized electrons and protons is calculated to order $\alpha^3$, retaining only the elastic intermediate state in the unitarity sum that occurs. The result is therefore expected to correspond closely to the physical situation for electron laboratory energies up to the region where pion production becomes important. Using the "dipole fit" for the proton form factors $G_E$ and $G_M$, the maximum value of the polarization is found to be $\sim 0.03\%$ for electron energies below 400 MeV. Above 10 GeV, the maximum elastic effect is $\sim 1\%$.

## I. INTRODUCTION

IN the one-photon-exchange approximation, the scattering of unpolarized electrons by an unpolarized proton target gives no polarization of the recoil proton (see Sec. II, for example). Any nonzero polarization of the recoil proton, transverse to the scattering plane, must arise from interference of higher-order amplitudes with the one-photon amplitude. We are interested in the contribution from the two-photon-exchange amplitudes of Fig. 1. There will be such diagrams for each

* Now at the California Institute of Technology, Pasadena, Calif. 91109.